

Microfluidic Concentration-Enhanced Single Cell Enzyme Activity Assay

by

Aniruddh Sarkar

M.Tech., Electrical Engineering, Indian Institute of Technology Bombay (2003)

B.Tech., Electrical Engineering, Indian Institute of Technology Bombay (2003)

Submitted to the Department of Electrical Engineering and Computer Science
in Partial Fulfillment of the Requirements for the Degree of

Doctor of Philosophy

at the

MASSACHUSETTS INSTITUTE OF TECHNOLOGY

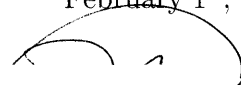
February 2013

© Massachusetts Institute of Technology 2013. All rights reserved.

Signature of Author.....

Department of Electrical Engineering and Computer Science

February 1st, 2013



Certified by.....



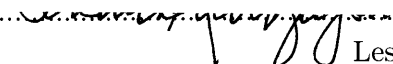
Jongyoon Han

Associate Professor of Electrical Engineering and Computer Science

Associate Professor of Biological Engineering

Thesis Supervisor

Accepted by.....



Leslie A. Kolodziej

Chairman, Department Committee on Graduate Students

Department of Electrical Engineering and Computer Science

Microfluidic Concentration-Enhanced Single Cell Enzyme Activity Assay

by

Aniruddh Sarkar

Submitted to the Department of Electrical Engineering and Computer Science
on February 1st 2012 in partial fulfillment of the
requirements for the degree of Doctor of Philosophy in
Electrical Engineering and Computer Science

Abstract

Cells sense stimuli, process information and respond using signaling networks regulated by enzymatic activity of various proteins. Aberrations in signaling are associated with diseases such as cancer. Most current methods lack the sensitivity to measure enzymatic activity in single cells and instead measure the average of large cell populations. Cellular heterogeneity, overlooked in these methods, is widespread and relevant. Microfabricated tools are uniquely suited to single cell analysis due to the match in size scale which enables high sensitivity, high throughput measurements.

In this thesis we develop a microfluidic platform for the direct measurement of enzyme activities from selected single cells without disrupting their extracellular context. We develop modules to: enhance enzyme assay sensitivity by microfluidic confinement, interface microfluidic devices with selected single cells, enable multiplexing and then integrate these modules to perform single cell assays.

We first investigate electrokinetic trapping of charged biomolecules in a nanofluidic concentrator for enhancing enzyme assay sensitivity by simultaneously accumulating enzyme and substrate into a reaction plug. Non-linear enhancement of reaction kinetics in this device is predicted by a mathematical model and experimentally verified. A linear enhancement mode is developed where only the enzyme is accumulated and is reacted with substrate later in an enclosed volume defined by integrated pneumatic valves or by micro-droplets formed using an integrated droplet generator. This device is then used to perform high-throughput measurement of secreted cellular proteases.

We then develop a microfluidic probe for lysis and capture of the contents of selected single adherent cells from standard tissue culture platforms by creating a small lysis zone at its tip using hydrodynamic confinement. The single cell lysate is then divided and mixed with different substrates and confined in small chambers for fluorimetric assays. An integrated nanofluidic concentrator enables further concentration-enhancement. We demonstrate the ability to measure, from selected single cells, the activity of kinases: Akt, MAPKAPK2, PKA and a metabolic enzyme, GAPDH - separately or simultaneously. This assay platform can correlate single cell phenotype or extracellular context to intracellular biochemical state. We present preliminary explorations of the correlation of cell morphology or local cell population density to kinase activity.

Thesis Supervisor: Jongyoon Han

Title: Associate Professor of Electrical Engineering and Computer Science and Associate Professor of Biological Engineering

Acknowledgement

In the course of my doctoral studies and research, I have definitely received much more than I have given – wisdom, knowledge, vision, ideas, guidance, encouragement, friendship and collegiality. My research advisor Prof. Jongyoon Han has been for me, a source of all of the above and more and I would like to extend my heartfelt gratitude to him for everything. I would like to thank the members of my thesis committee Profs. Douglas Lauffenburger, Scott Manalis and Joel Voldman. Their excellent and timely input of ideas, direction and quality checks has shaped this work and their encouragement has been essential in keeping me going.

Given the thoroughly interdisciplinary nature of this work, collaborators have been critical to its development. Dr. Sarah Koltz (Lauffenburger/Griffith Labs) was closely involved with the single cell kinase assay work since its inception and has been an equal contributor of ideas and effort and perhaps more importantly, has been great fun to work with. The droplet-integration idea was brought to fruition by Dr. Chia-Hung Chen and his intense motivation and excellent experimental skill were inspiring. I inherited the work of Drs. Jeonghoon Lee and Yong-Ak Song and would like to thank them for their efforts that went before me. The concentration-enhanced mobility shift kinase assay was developed and performed by Lih Feng Cheow, whom I would also like to thank for many stimulating discussions over the years that we were officemates.

I would like to thank all my fellow members of the Han lab – those who helped me get started: Jianping Fu, Ying-Chih Wang, Pan Mao; those whom I have worked with: Leon Li, Sha

Huang, Lidan Wu, Hyung-Wan Do and all others I have had the pleasure to interact with and learn from, over time including: Sung-Jae Kim, Hansen Bow, Rhokyun Kwak.

I would also like to thank members of the RLE 8th floor community for help at various points and members of Voldman and Yanik labs especially for sharing equipment and tips about their use. I would like to acknowledge staff members at MTL for help in microfabrication. I would also like to acknowledge the helpful discussions with members of the Cell Decision Processes (CDP) meetings, which also formed my primary source of exposure to exciting biological problems. I must acknowledge the generous financial support from the MIT CDP Center which was funded by NIH (P50-GM68762).

I would also like to take this opportunity to thank again my earlier mentors at IITB, Drs. Rakesh Lal and Ashutosh Shastry who provided the formative experiences that led me here. My old friends from IITB and the friends I found at MIT have formed my home away from home for all these years. I hope they will excuse my not listing them here by name and deed for they are too numerous and have been too generous to me.

None of this would have been possible without the unconditional love and support provided by my family and the sacrifices made by them. I am grateful to my parents who have always put my welfare above their own and given me the freedom and courage to pursue my dreams. I owe a special debt of gratitude to my wife, Debasmita for her understanding, support, love and all the sacrifices she made, especially over the last two years. I would like to dedicate this thesis to them.

Table of Contents

Chapter 1 Introduction	9
1.1 Looking at One among Many: A Role for Microfluidics and Nanofluidics in Biology	9
1.2 Single Cell Analysis	10
1.3 Thesis Scope and Structure	11
1.4 References.....	12
Chapter 2 Current Single Cell Analysis Methods and the Role of Microfluidics.....	13
2.1 Why Analyze Single Cells?	13
2.2 Single Cell Analysis: Conventional vs. Microfluidic Methods	16
2.3 Single Cell Genomic Analysis	17
2.4 Single Cell Proteomics.....	19
2.5 Single Cell Phenotype Characterization.....	24
2.6 Connecting Signals to Responses in Single Cells.....	25
2.7 References.....	26
Chapter 3 Non-Linear and Linear Enhancement of Enzymatic Reaction Kinetics using a Biomolecule Concentrator	31
3.1 Introduction.....	31
3.2 Experimental Methods.....	35
3.3 Reaction Kinetics Model and Simulation.....	38
3.4 Non-linear Enhancement Mode Experiments.....	43
3.5 Linear Enhancement Mode Experiments	47

3.6 Integration with Droplet-Based Microfluidics.....	51
3.7 Measurement of Activity of Secreted Matrix Metalloproteinases.....	53
3.8 Conclusions and Future Directions.....	56
3.9 References.....	58
Chapter 4 An Integrated Microfluidic Probe for Single Cell Kinase Activity Measurement.....	61
4.1 Introduction.....	61
4.2 Selective Single Cell Lysis.....	63
4.3 Integrated Microfluidic Probe v1.....	66
4.4 Optimization of Microfluidic Probe for Higher Sensitivity, Repeatability and Throughput	72
4.5 Integrated Microfluidic Probe v2: Measuring Kinase Activities from Multiple Single Cells	74
4.6 Single Cell Kinase Activity Measurements	77
4.7 Deconvolving Technical and Biological Variability in Single Cell Kinase Activity Measurements.....	81
4.8 Integrated Microfluidic Probe v3: Measuring Multiple Kinase Activities from Single Cells	83
4.9 Conclusions and Future Directions.....	85
4.10 References.....	87
Chapter 5 Conclusions and Future Work	89
5.1 Thesis Contributions	89
5.2 Directions for Future Work	91

Chapter 1 Introduction

The advancement of science, and arguably that of civilization itself, is linked to the development of novel tools as much as it is to that of new concepts and paradigms. The advent of the telescope made possible Galileo's observation of the phases of Venus which was among the most important in human history. Tycho Brahe's extensive and accurate compilation of astronomical observations enabled Kepler's derivation of a model for planetary motion which in turn was used by Newton in proposing the universal law of gravitation. Biology and medicine, today, can be argued to be at a similar point where scientists need tools for high throughput acquisition of information across levels of biological organization and across spatial and temporal scales.

1.1 Looking at One among Many: A Role for Microfluidics and Nanofluidics in Biology

Microfluidic and nanofluidic devices and systems by definition have a length scale ranging from a few nanometers to a few tens of micrometers which closely matches the length scale spanned by a range of bio-objects of interest from single macromolecules: DNA, RNA and proteins to single organelles to single cells. This match in length scales provides a unique opportunity for micro/nano-fluidics in terms of the **sensitivity** or **resolution** to study and manipulate single bio-objects instead of the large ensembles studied in traditional methods.

Microfabrication methods, borrowed from microelectronics, have the capability to integrate a very large number and variety of unit devices in a small integrated system at a very low extra cost per unit added. This creates the potential for microfluidic systems to achieve a high level of **automation** by integration of multiple operations in a modular fashion that would otherwise require laborious manual interventions and also very **high-throughput** in gathering data by cost-effective repetition of a number of identical systems on a single chip [1]. Both these features are of critical importance in studying single bio-objects in the large numbers and at the high speed necessary to obtain statistically significant results in the presence of heterogeneity.

The small size of these devices also gives rise to physical phenomena (such as laminar flow in microfluidic channels or ion concentration polarization at micro-nano interfaces [2]) unique to these length-scales which can be harnessed to enable new methods of sensing and manipulation of single bio-objects.

1.2 Single Cell Analysis

In cellular analysis it is increasingly realized [3-6] that while traditional ensemble average measurements (from 10^3 - 10^6 cells) have provided the bulk of information gathered in cell biology until recently, heterogeneity in individual cell constituents and behavior is in fact ubiquitous. This confounds understanding of biological mechanisms [4], has consequences for the treatment of diseases [5] and in fact, if studied along with the proper extracellular context, can be used as a tool to generate new understanding of cell behavior [6]. Microfluidic and nanofluidic devices and systems – due to the above-mentioned features of high sensitivity, throughput and

automation – are exceptionally well-suited to single cell analysis at various scales ranging from genes, gene transcripts, proteins, peptides and metabolites to whole cell phenotypic measures such as cell mass and motility.

1.3 Thesis Scope and Structure

While single cell genomics is relatively advanced [7] primarily due to the amplification and resultant sensitivity afforded by the Polymerase Chain Reaction (PCR), single cell proteomics is impeded by the low abundance of most cellular proteins, lack of an easy amplification scheme and consequent sensitivity bottlenecks which can be addressed by miniaturization.

This thesis seeks to develop an integrated microfluidic system-on-chip which can measure the activities of proteins, most prominently: kinases, from single adherent mammalian cells and enable the correlation of the single cell kinase activities with the extracellular context and cellular phenotype measurements. Due to their relative importance in human disease models, to be able to integrate our data with that from the wealth of existing studies and due to the hitherto persistent challenge in interfacing microfluidic systems to them, we focus on adherent cells in standard tissue culture platforms.

We begin with a survey of current single cell analysis methods and a critical comparison of traditional and microfluidic methods in Chapter 2. Chapter 3 presents the investigation of enhancement of enzymatic reaction kinetics using an electrokinetic bio-molecule concentrator and its integration with a valve-isolated reaction chamber or encapsulating droplets and their use to detect secreted cellular proteases. The development and optimization of a microfluidic

probe which measures intracellular kinase activities in selected single adherent cells is presented in Chapter 4 which is followed by a summary of this work and directions for future work in Chapter 5.

1.4 References

- [1] G. M. Whitesides, "The origins and the future of microfluidics," *Nature*, vol. 442, pp. 368-73, Jul 27 2006.
- [2] Y.-C. Wang, *et al.*, "Million-fold Preconcentration of Proteins and Peptides by Nanofluidic Filter," *Analytical Chemistry*, vol. 77, pp. 4293-4299, 2005.
- [3] S. J. Altschuler and L. F. Wu, "Cellular heterogeneity: do differences make a difference?," *Cell*, vol. 141, pp. 559-63, May 14 2010.
- [4] A. Loewer and G. Lahav, "We are all individuals: causes and consequences of non-genetic heterogeneity in mammalian cells," *Curr Opin Genet Dev*, vol. 21, pp. 753-8, Dec 2011.
- [5] M. Niepel, *et al.*, "Non-genetic cell-to-cell variability and the consequences for pharmacology," *Current Opinion in Chemical Biology*, vol. 13, pp. 556-561, 2009.
- [6] L. Pelkmans, "Cell Biology. Using cell-to-cell variability--a new era in molecular biology," *Science*, vol. 336, pp. 425-6, Apr 27 2012.
- [7] D. Wang and S. Bodovitz, "Single cell analysis: the new frontier in 'omics'," *Trends Biotechnol*, vol. 28, pp. 281-90, Jun 2010.

Chapter 2 Current Single Cell Analysis Methods and the Role of Microfluidics

2.1 Why Analyze Single Cells?

The cell is the fundamental unit of all known life and it is the central challenge of biology to understand how a cell processes information and responds to perturbations. Most of our understanding of the cell is obtained from bulk measurements made on large populations of cells. This is to some extent due to a focus on finding mechanisms common to most cells but also largely due to technical limitations of conventional methods in making measurements from the very limited amount of starting material available in a single cell (usually ~5-10pg of DNA/RNA, ~1ng of total protein in a single human cell).

Misleading Population Averages

Cellular heterogeneity has been found to be widespread in nature and the extent to which bulk average measurements link faithfully to individual cell behavior is increasingly doubted in a variety of contexts as discussed in a number of recent reviews [1-3]. Population averages may not represent individual cells function even for a normal distribution of single-cell measurements (Figure 2.1a). For example, subpopulations of clonally derived hematopoietic progenitor cells with low or high expression of the stem cell marker Sca-1 were seen to give rise to different blood cell lineages [4]. In the presence of rare or small subpopulations (Figure 2.1b), population averages can represent the vast majority of cells and still miss important biology.

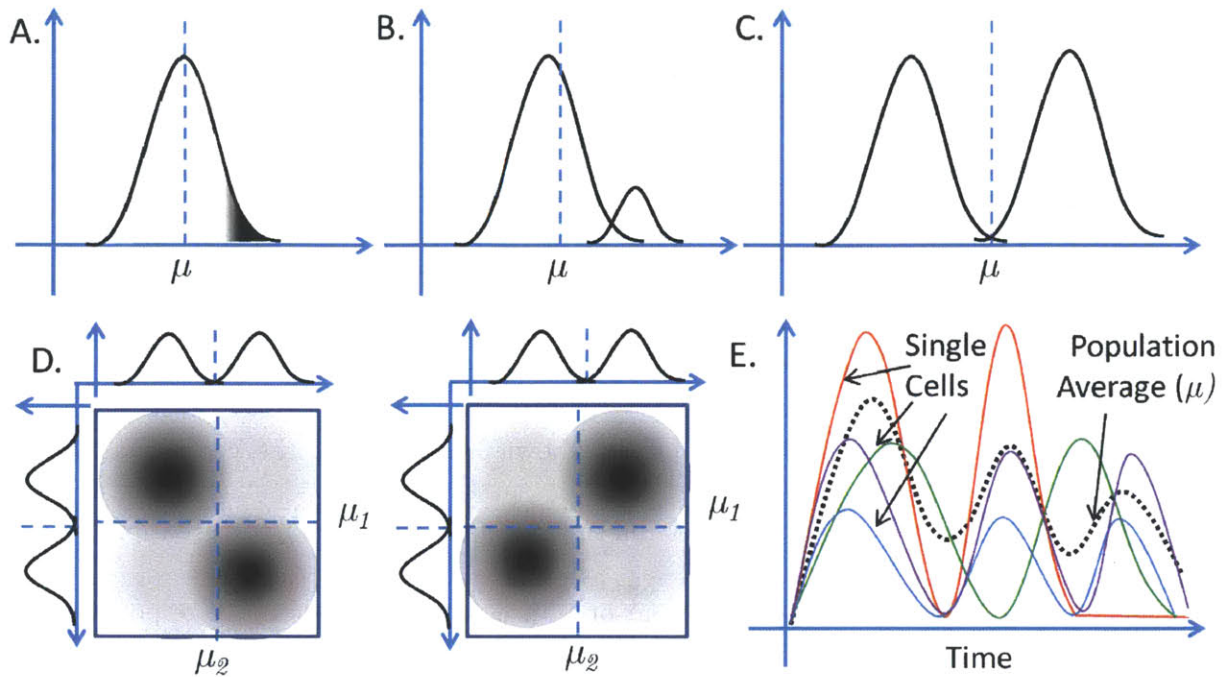


Figure 2.1. Population averages hide cellular heterogeneity. **a.** Behavior of cells far away from the mean or **b.** small subpopulations may not be captured by the mean. **c.** For a bimodal population the mean may not capture behavior of any cells. **d.** Correlated and anti-correlated variables maybe difficult to distinguish by average measurements and simultaneous multi-parameter single cell measurements are needed to resolve this. **e.** Asynchronous dynamics of single cells (variable number and phase of constant-amplitude pulses here) can lead to misleading population-averaged dynamics measurements (damped pulses here).

For example, in cancer, subpopulations of cells have been found to contribute unequally to disease progression and the “cancer stem cell” hypothesis arising from this is a subject of debate [5]. When a cell population contains several dominant, distinct subpopulations, the ensemble average may not represent the majority of cells or even any single cell (Figure 2.1c). This has been seen in presence of “all-or-nothing” responses with variations in the threshold across the population – such as in hormone induction of maturation in *Xenopus* oocytes – which can be misinterpreted as a graded response in bulk measurements.

For elucidating signaling networks, the situation can get especially complicated as the monitoring of multiple components is often essential [6] but in presence of heterogeneity,

correlation and anti-correlation among different measurands may be difficult to distinguish in bulk average measurements (Figure 2.1d) [7]. Additionally, the true dynamics of a signaling network can be hidden by lack of synchronicity among cells (Figure 2.1e) [8] and lead to wrong mechanistic interpretations.

Sources of Cellular Heterogeneity

Heterogeneity among cells can emerge from fluctuations in internal components of cells which occur due to the discrete nature of basic cellular processes. For example, fluctuations in regulatory proteins, have been shown to determine the probability and timing of ligand-induced apoptosis [9]. Heterogeneity in cellular response can also arise from differences in intrinsic cellular states such as cell-cycle phase. For example, pulses of the tumor suppressor p53 in appear to happen spontaneously in un-synchronized, proliferating cells but were found to be correlated with DNA replication which causes intrinsic damage [10]. Heterogeneity of cellular response can also be due to the variations in the microenvironment of a cell. The population context of a cell such as local cell density, number of cell-cell contacts etc can vary dramatically between individual cells. For example, these parameters have been shown to influence the susceptibility for viral infection [11].

Appropriately chosen single cell measurement techniques can be useful in presence of any of the above sources of heterogeneity and can resolve each of the above issues with bulk average measurements. Additionally, single cell techniques also lend themselves naturally to analyzing scarce and/or mixed yet difficult to sort cell samples such as adult stem cells or other heterogeneous primary tissue samples. Also most environmental samples may contain a majority

of uncultivable species of microbes and the ability to isolate individual cells and analyze them can help probe such biological “dark matter” [12, 13].

2.2 Single Cell Analysis: Conventional vs. Microfluidic Methods

An increasing number of works have appeared in recent years focusing on single cell analysis as summarized in multiple recent reviews [14-17]. Single cells can be studied at multiple levels: from the population context of single cells to single cell phenotypic/functional measurements to underlying proteins: their levels, localization and activity in single cells to the sequencing of DNA and its expression as RNA in single cells. Additionally, various metabolites and other small molecules can also be quantified in single cells. Ideally, one would like to correlate diverse cellular phenotypes to the differences in underlying biochemistry and hence discover the mechanistic basis of the observed heterogeneity.

Microfluidic systems – due to their size scale and associated phenomena – are uniquely suited to single cell manipulation and analysis because of potential advantages in sensitivity, throughput and automation. Various microfluidic devices and systems have been developed over the last decade, targeted at various aspects of single cell analysis which have been the subject of some recent reviews. [15, 16, 18]. Various tools based on conventional technologies also exist or are being actively developed for most of the above measurement levels. Given the relative familiarity of biologists with these tools, microfluidics systems have to compete with these traditional tools by delivering unique and/or complementary advantages in gathering various kinds of single cell data and placing them in context of existing knowledge. In the rest of this chapter, we seek to critically review the relative advantages of microfluidic tools relative to

available traditional tools at the various levels of single cell analysis and also propose some technology gaps/opportunities for microfluidic systems. While heterogeneity has been found to be common and is widely studied using single cell techniques in bacteria and yeast, we focus here on mammalian single cell analysis.

2.3 Single Cell Genomic Analysis

A single cell usually contains less than 10pg of nucleic acid material. Yet, driven mostly by the exponential, selective amplification afforded by PCR and its variants, single cell sequencing and gene expression analysis is the most advanced among single cell analysis methods. An excellent review of the evolution and current status of single cell genomic analysis has appeared recently [19].

Single Cell PCR Amplification Based Methods

The analysis of DNA [20] and RNA from single cells [21, 22] has been reported, starting as early as 1980s. Quantitative reverse transcriptase PCR (qRT-PCR or qPCR), which couples reverse transcription and incorporation of a fluorescent tag, allows sensitive measurement down to single molecule range and analysis of many ($\sim 3-4$) genes is possible from the same sample. This technique has been used to analyze gene expression in a single cell [23]. Microarrays allow the measurement of thousands of genes at once using hybridization of labeled sample to an array of probes but typically require 1-2 μ g of mRNA. By using PCR to amplify mRNA from single cells up to this amount, microarray analysis of single cells has been performed [24]. Using next generation sequencing technologies, mRNA sequencing (mRNA-Seq) protocols have been developed for single cell whole transcriptome analysis [25]. Also sequencing of the genome of

single *E. Coli* cells after amplification using multiple displacement amplification (MDA) has been demonstrated [26].

Issues and avenues for optimization in further application of many of the above amplification based techniques are: increasing sensitivity and precision by dealing with the introduction of bias/errors or contamination in the amplification step and increasing throughput in terms of number of cells and genes by automation and multiplexing. Microfluidic techniques using large numbers of micro-reactors in the form of either chambers with pneumatic valves [27] or water-in-oil droplets [28] have been applied for increasing sensitivity and throughput of PCR. The small volume of the reactor provides a concentration-enhancement and leads to a higher initial template concentration which can improve amplification bias/error issues [29] and make it easier to implement digital PCR (dPCR) [30] where direct counting of single starting molecules after stochastic encapsulation and amplification. The throughput and ease of use of PCR-based methods is significantly improved by microfluidic automation and parallelization as such devices can help automating and integrating on a single chip, various steps ranging from single cell isolation from complex environmental or tissue samples [13, 31] to the combinatorial mixing of thousands of PCR reactions in parallel [32] while decreasing the risk of contamination.

The unique low volume manipulation capabilities of microfluidics in PCR were also recently demonstrated in isolating and amplifying single chromosomes from a single cell thus enabling haplotyping of single cells [33].

Microscopy Based Methods

A common disadvantage with the PCR-based methods is the loss of the tissue or other extracellular context information as single cells are usually suspended and isolated for lysis and DNA extraction. This can be mitigated by microscopy based approaches which have been developed to visualize nucleic acids in single cells. RNA fluorescent in-situ hybridization uses fluorescently tagged probes to mark mRNA molecules in fixed cells [34] and has been used to count individual mRNA molecules in single cells and study cell-cell variability [35]. Microscopy can be used to understand the spatial relationships between different cells and correlate the cell-cell variability with the extracellular context of individual cells.

A limitation in microscopy-based methods stems from its usually limited throughput. These limitations can be overcome by automated microscopy aided by automated microfluidic parallelization of cell growth/treatment conditions [36]. mRNA FISH has been applied to thousands of single bacterial cells using an automated microfluidic device [37].

2.4 Single Cell Proteomics

A single mammalian cell contains up to 1ng of total protein but with a large dynamic range in abundances of the large number of different proteins ranging from a few copies to up to 10^5 copies which makes single cell proteomic measurement much more challenging. However, significant non-genetic sources of heterogeneity exist downstream of gene expression in mammalian cells at translational and post-translational levels [2, 38] which cannot be probed in single cell genomic analysis methods. Information at the protein level more closely approaches

signaling events. Direct reads of protein abundance, localization within the cell and protein activity at the single cell level are essential in understanding such cellular heterogeneity.

Protein Abundance and Localization

Techniques for measuring proteins in single cells usually work by labeling specific proteins for visualization and/or measurement. The labeling techniques can be broadly classified as those using tagged antibodies against proteins and those using genetic manipulation of cells to express proteins fused with specific fluorescent proteins. Antibody-based techniques usually work with fixed cells for intracellular proteins and hence at single time points or with surface markers on live cells. Antibodies can be used to measure the level of phosphorylated forms of proteins which can be used as a surrogate for protein activity although this correlation might break down in presence of multiple post-translational modifications [39]. Antibody-based methods in general, are also limited by the quality of antibodies available in terms of their sensitivity and cross-reactivity. Fluorescent-tagged proteins can be used in live cells which can be tracked over time. Generating cells expressing fluorescent-tagged proteins can be a laborious process and the addition of the fluorescent protein tag can hinder normal protein function.

Visualization or measurement of the protein is usually done by either microscopy or flow cytometry. Microscopy can provide protein levels as well as intracellular localization information and with live-cell imaging can provide temporal information as well while maintaining the tissue context of the cell and providing information about the population and other extracellular context of the single cell. But it usually works at a relatively low throughput. Flow cytometry usually provides only protein abundance information and at a single time-point at a time but

works at a high throughput and can probe a large number of single cells quickly. With fluorescent tagging, the number of simultaneous parameter measurements (usually ~ 12 maximum) is limited by the spectral overlap of fluorophores, independent of the detection method. Recent development of mass-based flow cytometry [40] which uses lanthanide tags on antibodies and time-of-flight mass spectrometry for measurement enables much higher degree of multiplexing and up to 34 simultaneous parameter measurements have been demonstrated [41].

Microfluidic platforms have been developed for single cell analysis based on microscopy. High throughput imaging of protein levels, localization and dynamics in single cells can be facilitated by microfluidic platforms [36, 37, 42] which help in automating the growth, treatment and imaging of single cells. Isolation suspended single cells in microfabricated wells [43] has enabled single cell measurement of secreted proteins and the isolation of cells producing specific proteins such as antibodies. Isolation of suspended single cells in valved microfluidic chambers and the capture of secreted proteins [44] or intracellular proteins and their phosphorylated forms after cell lysis [45, 46] on to a barcoded pattern of a DNA-encoded antibody library in an adjacent microfluidic chamber has been demonstrated. The spatial separation of the antibody binding sites in these techniques can ease the limitations posed by spectral overlap of fluorophores and cross-reactivity of antibodies. A microfluidic flow cytometry method using droplet encapsulation of single cells has been developed that can be used for enzyme-amplified detection of low-abundance cell-surface biomarkers [47]. A parallel microfluidic imaging cytometer has been demonstrated which combines the high throughput of flow cytometry with the access to higher information content afforded by imaging [48].

Protein Activity

Measurement of protein activity in single cells is extremely valuable as it provides the most direct access to actions taking place inside the cell and is usually the closest link to function. A large fraction of active proteins of interest in the cellular signaling network are kinases which work by adding phosphate groups to their substrates. Protein activity is usually measured using synthetic or natural substrates of the target protein such as peptides or protein fragments or proteins whose measurable properties such as radioactivity, fluorescence or charge change on reacting with it. For secreted or cell-surface proteins this reaction can take place outside the cell while for most intracellular proteins either the substrate has to be introduced into the cell or the cell has to be lysed before the reaction can happen.

Genetically encoded FRET sensors allow kinase activities to be monitored over time in single live cells [49]. The challenges in this method are the limited multiplexing abilities and the requirement for genetic manipulation of cells. Fluorescently-tagged kinase substrate peptides have been introduced into cells by microinjection and the reaction products and un-reacted substrates were later separated in a mobility-shift assay by capillary electrophoresis of the single cell lysate, enabling the measurement of three kinase activities from a single adherent mammalian cell at single time points in each experiment [50]. In rare cases, such peptides can be naturally cell-membrane permeable [51] or in other cases, they can be made so by attaching a hydrophobic chain such as the myristoyl group [52]. Overall, this method is limited by challenges in achieving specificity of the reaction in the intracellular milieu and the susceptibility of the peptides to non-specific cleavage by intracellular proteases [53].

Most conventional protein activity measurement methods work with cell lysates and as end-point measurements. Protocols based on the measurement of radioactivity after reacting crude or immuno-affinity purified cell lysates with [γ - ^{32}P]ATP are most common for kinase activity measurement [54]. A homogenous fluorescence-based assay for protein kinase activity in cell lysates has been developed which uses fluorogenic substrate peptides [55] and avoids the relatively cumbersome use of radioactivity.

These methods are usually unable to measure single cell protein activity directly as they require relatively large ($\sim\mu\text{g}$ -scale) amounts of protein for measurable activity in the relatively large assay volumes ($\sim 50\mu\text{L}$ or more) used in traditional reaction formats. This presents an opportunity for microfluidic tools as a simple reduction in reaction volume can be used to approach single cell sensitivity in these methods. The measurement of kinase activity from small amounts of patient samples using a miniaturization of the radioactive kinase assay has been demonstrated but this method still requires up to 3000 cells [56]. Measurement of kinase activity from cell lysate equivalent to that from ~ 4 -5 cells was demonstrated [57] using fluorogenic peptide substrates with a nanofluidic biomolecular concentrator [58] to gather molecules into a $\sim\text{pL}$ -scale plug on chip. Work is also in progress to use the biomolecular concentrator with fluorescently labeled peptides to perform a single cell concentration-enhanced mobility shift kinase assay [59]. Cell trap arrays have been used to isolate single suspended cells and assay the activity of intracellular carboxylesterases for which cell-permeant substrates are commonly available [51]. Microchamber arrays with cell traps and have been used to trap and lyse single

suspended cells and analyse the level of intracellular metabolites and the activity of a house-keeping enzyme G6PDH [60].

2.5 Single Cell Phenotype Characterization

Single cell phenotype can be quantified in a number of ways. Individual cell behavior such as migration, proliferation and morphological changes can be considered part of cellular phenotype. Depending on the context, some features discussed above (protein secretion or cell-surface markers) could also be considered aspects of phenotype. Direct observation using live-cell microscopy is the most common method for direct single cell phenotype characterization. For direct measurement of the cellular phenotype in the natural extracellular context, methods for intra-vital imaging have been developed [61]. Measurement of other parameters of the single cell such as mass/density, chemical, mechanical or optical properties can sometimes be used to indirectly make phenotypic measurements.

Microsystems have been used to facilitate high throughput phenotypic characterization by automating microscopy-based methods [36, 62, 63] with or without isolation of single cells as described for above modes of single cell analysis. Microsystems can also enable unique measurements due to their sensitivity such as single cell mass [64, 65] and density measurements [66] which would otherwise be impossible. Microsystems can also be used to mimic the natural extracellular context [67] in which the cellular phenotype of interest such as cell migration is displayed and thus enable measurement of the phenotype which can be closer to the in-vivo phenotype.

2.6 Connecting Signals to Responses in Single Cells

In order to elucidate the underlying mechanisms of cellular heterogeneity, it is important to be able integrate the above modes of single cell analysis and create a link from the extracellular and population context of the single cell to phenotypic measurements to protein and gene level measurements. In heterogeneous cell populations, this would be best accomplished if the phenotype measurement and the signaling measurements can be performed on the same cell simultaneously.

Phenotypic measurements typically require maintaining the measurement context relatively similar to the natural context in which the cell behavior of interest would occur. For example, the proliferation of an adherent cell type requires, at the very minimum, adhesion to a surface and may require a certain minimum cell density or even cell-cell contact. Similarly cell migration is also an adherent cell phenotype. However the measurement of cell surface or intracellular proteins using flow cytometry would require disrupting cell adhesion to make a single cell suspension. Such practical experimental limitations in existing techniques mean that often phenotypic measurements are made separately from signaling measurements making it difficult to correlate them at the single-cell level.

Microfluidics can help in recreating complex extracellular environments in-vitro, as demonstrated in recent ‘organ-on-chip’ work [68, 69], and thus help in systematically exploring the effect of cell-cell interactions and population-level parameters on single cell phenotypic variability. Microfluidic systems also offer unique single cell sensing and manipulation capabilities and the possibility to integrate them seamlessly in a single system-on-chip, thus

presenting an opportunity to perform phenotypic and signaling measurements from the same single cell. Thus, with the development of appropriate integrated cell culture, single cell manipulation and measurement platforms, an integrative study linking cellular heterogeneity to population context and to intracellular biochemistry can be performed.

Alternatively, a single cell analysis platform which integrates standard, well-studied platforms for performing single cell phenotypic measurements such as 2-D or 3-D tissue culture with microfluidic devices for selective single cell biochemical analysis can also enable integrative studies of cellular heterogeneity. Such platforms will provide new insights into the cellular mechanisms and indeed help better understand and combat disease mechanisms.

2.7 References

- [1] S. J. Altschuler and L. F. Wu, "Cellular heterogeneity: do differences make a difference?," *Cell*, vol. 141, pp. 559-63, May 14 2010.
- [2] M. Niepel, *et al.*, "Non-genetic cell-to-cell variability and the consequences for pharmacology," *Current Opinion in Chemical Biology*, vol. 13, pp. 556-561, 2009.
- [3] B. Snijder and L. Pelkmans, "Origins of regulated cell-to-cell variability," *Nat Rev Mol Cell Biol*, vol. 12, pp. 119-25, Feb 2011.
- [4] H. H. Chang, *et al.*, "Transcriptome-wide noise controls lineage choice in mammalian progenitor cells," *Nature*, vol. 453, pp. 544-7, May 22 2008.
- [5] R. J. Gilbertson and T. A. Graham, "Cancer: Resolving the stem-cell debate," *Nature*, vol. 488, pp. 462-3, Aug 23 2012.
- [6] K. Sachs, *et al.*, "Causal protein-signaling networks derived from multiparameter single-cell data," *Science*, vol. 308, pp. 523-9, Apr 22 2005.
- [7] L. H. Loo, *et al.*, "An approach for extensively profiling the molecular states of cellular subpopulations," *Nat Methods*, vol. 6, pp. 759-65, Oct 2009.
- [8] G. Lahav, *et al.*, "Dynamics of the p53-Mdm2 feedback loop in individual cells," *Nature Genetics*, vol. 36, pp. 147-150, 2004.
- [9] S. L. Spencer, *et al.*, "Non-genetic origins of cell-to-cell variability in TRAIL-induced apoptosis," *Nature*, vol. 459, pp. 428-432, 2009.
- [10] A. Loewer, *et al.*, "Basal dynamics of p53 reveal transcriptionally attenuated pulses in cycling cells," *Cell*, vol. 142, pp. 89-100, Jul 9 2010.

- [11] B. Snijder, *et al.*, "Population context determines cell-to-cell variability in endocytosis and virus infection," *Nature*, vol. 461, pp. 520-523, 2009.
- [12] D. Wu, *et al.*, "Stalking the fourth domain in metagenomic data: searching for, discovering, and interpreting novel, deep branches in marker gene phylogenetic trees," *PLoS One*, vol. 6, p. e18011, 2011.
- [13] Y. Marcy, *et al.*, "Dissecting biological "dark matter" with single-cell genetic analysis of rare and uncultivated TM7 microbes from the human mouth," *Proc Natl Acad Sci U S A*, vol. 104, pp. 11889-94, Jul 17 2007.
- [14] D. Wang and S. Bodovitz, "Single cell analysis: the new frontier in 'omics'," *Trends Biotechnol*, vol. 28, pp. 281-90, Jun 2010.
- [15] V. Lecaute, *et al.*, "Microfluidic single cell analysis: from promise to practice," *Curr Opin Chem Biol*, vol. 16, pp. 381-90, Aug 2012.
- [16] H. Yin and D. Marshall, "Microfluidics for single cell analysis," *Curr Opin Biotechnol*, vol. 23, pp. 110-9, Feb 2012.
- [17] V. K. Rajasekhar, *et al.*, "Single-Cell Approaches to Dissect Cellular Signaling Networks," in *Regulatory Networks in Stem Cells*, ed: Humana Press, 2009, pp. 337-345.
- [18] C. E. Sims and N. L. Allbritton, "Analysis of single mammalian cells on-chip," *Lab on a Chip*, vol. 7, pp. 423-440, 2007.
- [19] T. Kalisky, *et al.*, "Genomic analysis at the single-cell level," *Annu Rev Genet*, vol. 45, pp. 431-45, 2011.
- [20] H. H. Li, *et al.*, "Amplification and analysis of DNA sequences in single human sperm and diploid cells," *Nature*, vol. 335, pp. 414-7, Sep 29 1988.
- [21] J. Eberwine, *et al.*, "Analysis of gene expression in single live neurons," *Proc Natl Acad Sci U S A*, vol. 89, pp. 3010-4, Apr 1 1992.
- [22] S. A. Mackler, *et al.*, "Stimulus-induced coordinate changes in mRNA abundance in single postsynaptic hippocampal CA1 neurons," *Neuron*, vol. 9, pp. 539-48, Sep 1992.
- [23] K. Taniguchi, *et al.*, "Quantitative analysis of gene expression in a single cell by qPCR," *Nat Methods*, vol. 6, pp. 503-6, Jul 2009.
- [24] M. K. Chiang and D. A. Melton, "Single-cell transcript analysis of pancreas development," *Dev Cell*, vol. 4, pp. 383-93, Mar 2003.
- [25] F. Tang, *et al.*, "mRNA-Seq whole-transcriptome analysis of a single cell," *Nat Methods*, vol. 6, pp. 377-82, May 2009.
- [26] K. Zhang, *et al.*, "Sequencing genomes from single cells by polymerase cloning," *Nat Biotechnol*, vol. 24, pp. 680-6, Jun 2006.
- [27] M. A. Unger, *et al.*, "Monolithic Microfabricated Valves and Pumps by Multilayer Soft Lithography," *Science*, vol. 288, pp. 113-116, April 7, 2000 2000.
- [28] T. Thorsen, *et al.*, "Dynamic Pattern Formation in a Vesicle-Generating Microfluidic Device," *Physical Review Letters*, vol. 86, pp. 4163-4166, 2001.
- [29] A. K. White, *et al.*, "High-throughput microfluidic single-cell RT-qPCR," *Proc Natl Acad Sci U S A*, vol. 108, pp. 13999-4004, Aug 23 2011.
- [30] L. Warren, *et al.*, "Transcription factor profiling in individual hematopoietic progenitors by digital RT-PCR," *Proc Natl Acad Sci U S A*, vol. 103, pp. 17807-12, Nov 21 2006.

- [31] P. C. Blainey, *et al.*, "Genome of a low-salinity ammonia-oxidizing archaeon determined by single-cell and metagenomic analysis," *PLoS One*, vol. 6, p. e16626, 2011.
- [32] J. Liu, *et al.*, "Solving the "world-to-chip" interface problem with a microfluidic matrix," *Anal Chem*, vol. 75, pp. 4718-23, Sep 15 2003.
- [33] H. C. Fan, *et al.*, "Whole-genome molecular haplotyping of single cells," *Nat Biotechnol*, vol. 29, pp. 51-7, Jan 2011.
- [34] A. Raj, *et al.*, "Imaging individual mRNA molecules using multiple singly labeled probes," *Nat Methods*, vol. 5, pp. 877-9, Oct 2008.
- [35] A. Raj, *et al.*, "Stochastic mRNA synthesis in mammalian cells," *PLoS Biol*, vol. 4, p. e309, Oct 2006.
- [36] R. Cheong, *et al.*, "High content screening in microfluidic devices," *Expert Opin Drug Discov*, vol. 5, pp. 715-720, Aug 1 2010.
- [37] Y. Taniguchi, *et al.*, "Quantifying E. coli proteome and transcriptome with single-molecule sensitivity in single cells," *Science*, vol. 329, pp. 533-8, Jul 30 2010.
- [38] A. Loewer and G. Lahav, "We are all individuals: causes and consequences of non-genetic heterogeneity in mammalian cells," *Curr Opin Genet Dev*, vol. 21, pp. 753-8, Dec 2011.
- [39] N. Kumar, *et al.*, "Quantitative analysis of Akt phosphorylation and activity in response to EGF and insulin treatment," *Biochemical and Biophysical Research Communications*, vol. 354, pp. 14-20, 2007.
- [40] D. R. Bandura, *et al.*, "Mass cytometry: technique for real time single cell multitarget immunoassay based on inductively coupled plasma time-of-flight mass spectrometry," *Anal Chem*, vol. 81, pp. 6813-22, Aug 15 2009.
- [41] S. C. Bendall, *et al.*, "Single-cell mass cytometry of differential immune and drug responses across a human hematopoietic continuum," *Science*, vol. 332, pp. 687-96, May 6 2011.
- [42] S. Tay, *et al.*, "Single-cell NF-kappaB dynamics reveal digital activation and analogue information processing," *Nature*, vol. 466, pp. 267-71, Jul 8 2010.
- [43] J. C. Love, *et al.*, "A microengraving method for rapid selection of single cells producing antigen-specific antibodies," *Nat Biotech*, vol. 24, pp. 703-707, 2006.
- [44] C. Ma, *et al.*, "A clinical microchip for evaluation of single immune cells reveals high functional heterogeneity in phenotypically similar T cells," *Nat Med*, vol. 17, pp. 738-43, Jun 2011.
- [45] Q. Shi, *et al.*, "Single-cell proteomic chip for profiling intracellular signaling pathways in single tumor cells," *Proc Natl Acad Sci U S A*, vol. 109, pp. 419-24, Jan 10 2012.
- [46] Y. S. Shin, *et al.*, "Chemistries for patterning robust DNA microbarcodes enable multiplex assays of cytoplasm proteins from single cancer cells," *Chemphyschem*, vol. 11, pp. 3063-9, Oct 4 2010.
- [47] H. N. Joensson, *et al.*, "Detection and analysis of low-abundance cell-surface biomarkers using enzymatic amplification in microfluidic droplets," *Angew Chem Int Ed Engl*, vol. 48, pp. 2518-21, 2009.

- [48] B. K. McKenna, *et al.*, "A parallel microfluidic flow cytometer for high-content screening," *Nat Methods*, vol. 8, pp. 401-3, May 2011.
- [49] C. M. Welch, *et al.*, "Imaging the coordination of multiple signalling activities in living cells," *Nat Rev Mol Cell Biol*, vol. 12, pp. 749-56, Nov 2011.
- [50] G. D. Meredith, *et al.*, "Measurement of kinase activation in single mammalian cells," *Nature Biotechnology*, vol. 18, pp. 309-312, 2000.
- [51] D. Di Carlo, *et al.*, "Single-Cell Enzyme Concentrations, Kinetics, and Inhibition Analysis Using High-Density Hydrodynamic Cell Isolation Arrays," *Analytical Chemistry*, vol. 78, pp. 4925-4930, 2006.
- [52] A. R. Nelson, *et al.*, "Myristoyl-based transport of peptides into living cells," *Biochemistry*, vol. 46, pp. 14771-81, Dec 25 2007.
- [53] A. Proctor, *et al.*, "Metabolism of peptide reporters in cell lysates and single cells," *Analyt*, vol. 137, pp. 3028-38, Jul 7 2012.
- [54] C. J. Hastie, *et al.*, "Assay of protein kinases using radiolabeled ATP: a protocol," *Nat Protoc*, vol. 1, pp. 968-71, 2006.
- [55] M. D. Shults, *et al.*, "A multiplexed homogeneous fluorescence-based assay for protein kinase activity in cell lysates.," *Nature Methods*, vol. 2, pp. 277-283, 2005.
- [56] C. Fang, *et al.*, "Integrated microfluidic and imaging platform for a kinase activity radioassay to analyze minute patient cancer samples," *Cancer Res*, vol. 70, pp. 8299-308, Nov 1 2010.
- [57] J. H. Lee, *et al.*, "Microfluidic Concentration-Enhanced Cellular Kinase Activity Assay," *Journal of the American Chemical Society*, vol. 131, pp. 10340-10341, 2009.
- [58] Y.-C. Wang, *et al.*, "Million-fold Preconcentration of Proteins and Peptides by Nanofluidic Filter," *Analytical Chemistry*, vol. 77, pp. 4293-4299, 2005.
- [59] L. F. Cheow, *et al.*, "Concentration-enhanced mobility shift assays with applications to aptamer-based biomarker detection and kinase profiling," in *15th International Conference on Miniaturized Systems for Chemistry and Life Sciences (μ TAS 2011)*, Seattle, USA, 2011, pp. 1023-1025.
- [60] K. Eyer, *et al.*, "A microchamber array for single cell isolation and analysis of intracellular biomolecules," *Lab Chip*, vol. 12, pp. 765-72, Feb 21 2012.
- [61] S. Giampieri, *et al.*, "Localized and reversible TGF β signalling switches breast cancer cells from cohesive to single cell motility," *Nat Cell Biol*, vol. 11, pp. 1287-96, Nov 2009.
- [62] V. Lecault, *et al.*, "High-throughput analysis of single hematopoietic stem cell proliferation in microfluidic cell culture arrays," *Nat Methods*, vol. 8, pp. 581-6, Jul 2011.
- [63] S. Gobaa, *et al.*, "Artificial niche microarrays for probing single stem cell fate in high throughput," *Nat Methods*, vol. 8, pp. 949-55, Nov 2011.
- [64] T. P. Burg, *et al.*, "Weighing of biomolecules, single cells and single nanoparticles in fluid," *Nature*, vol. 446, pp. 1066-9, Apr 26 2007.
- [65] M. Godin, *et al.*, "Using buoyant mass to measure the growth of single cells," *Nat Methods*, vol. 7, pp. 387-90, May 2010.
- [66] W. H. Grover, *et al.*, "Measuring single-cell density," *Proc Natl Acad Sci U S A*, vol. 108, pp. 10992-6, Jul 5 2011.

- [67] W. J. Polacheck, *et al.*, "Interstitial flow influences direction of tumor cell migration through competing mechanisms," *Proc Natl Acad Sci U S A*, vol. 108, pp. 11115-20, Jul 5 2011.
- [68] D. Huh, *et al.*, "Reconstituting organ-level lung functions on a chip," *Science*, vol. 328, pp. 1662-8, Jun 25 2010.
- [69] H. J. Kim, *et al.*, "Human gut-on-a-chip inhabited by microbial flora that experiences intestinal peristalsis-like motions and flow," *Lab Chip*, vol. 12, pp. 2165-74, Jun 21 2012.

Chapter 3 Non-Linear and Linear Enhancement of Enzymatic Reaction Kinetics using a Biomolecule Concentrator

3.1 Introduction

Enzyme catalyzed reactions are ubiquitous in nature and enzyme assays and the study of enzyme kinetics are essential in a wide range of scientific and technological domains such as biochemistry, medical diagnosis and biochemical engineering. Well-established methods for enzyme reactions such as microtiter-plate based colorimetric and fluorimetric assays usually require large sample volumes ($\sim 100\mu\text{L}$) and use relatively large amounts of the enzyme ($\sim 1\text{ng}$) per reaction. This presents a significant bottleneck in studying the kinetics of enzymes from precious samples such as those obtained directly from patients as well as from very low concentration samples such as a lysate from a single or a few cells. Monitoring the activities of various protein kinases, which play key roles in the cell signaling network, in single cells can help in understanding the heterogeneity in their levels in cell populations [1]. Such cellular heterogeneity, which cannot be studied by the usual ensemble average measurements, is thought to cause incomplete sensitivity to chemotherapy in cancer [2, 3]. However none of the frequently used methods provide the sensitivity needed to measure activities from molecules contained in a

single cell, especially once they are diluted in a volume ($\sim 1\mu\text{L}$) that can be physically handled by micropipettes [4].

Microfluidic systems significantly reduce required sample volume and assay time and also increase throughput of biochemical assays in general. Microfluidic enzyme kinetics studies that explore these opportunities have been reviewed earlier [5]. Homogeneous reactions using reactants mixing while in flow [6, 7] or with stationary reactants mixed in isolated chambers [8] or in water-in-oil droplets [9]. In addition, heterogeneous reactions using surface-immobilized enzymes [10] or gel-immobilized enzymes [11] have also been studied in microfluidic systems.

Most microfluidic approaches to enzyme kinetics successfully reduce the sample volume required but still have limitations in terms of the minimum enzyme concentration/activity they can probe. This is due to unfavorable scaling stemming from the limited reaction volumes in these devices. The optical path length available in these devices for use with any optical detection method is at least an order of magnitude lower ($\sim 10\mu\text{m}$ - $50\mu\text{m}$ typically) than that in a micro-titer plate ($\sim 1\text{mm}$ or more). The high surface to volume ratio in microfluidics also results in relatively high non-specific surface-binding reactions, which can compete with or even overshadow the bulk reaction rate in very low volumes. Also, when using small sample volumes and with low analyte concentrations, the statistical variation in number of enzyme molecules in a given volume can be significant resulting in irreproducible results.

Our group has earlier demonstrated a novel nanofluidic concentrator [12] that can be used to collect and trap charged molecules from a larger sample volume (~ 1 - $10\mu\text{L}$) into very small volume plugs (~ 10 - 100pL) on chip using the electric field gradient formed due to ion

concentration polarization [13] at the interface of a microchannel and a nanochannel[12] or nanoporous membrane [14] across which a voltage is applied. This technique can be used to tackle the above mentioned scaling problems in microfluidics as it results in a large increase in the local analyte concentration. Previously, we have employed such concentration-enhanced assays for protein immunoassay [15] and enzyme assays [14, 16] yielding significant (~100-1000 fold) sensitivity gains without changing the biochemistry involved (eg. quality of antibody) in the assay. In enzyme assays, the enhancement was obtained by mixing the sample with the target enzyme and a fluorogenic substrate off-chip and then trapping both molecules from the mixture into such a plug on the chip using the concentrator [14]. In these devices, the operation scheme of which is depicted in Figure 3.1a, at the very low enzyme concentrations of interest, a significant reaction rate is observed only in the trapped plug. This plug, in effect, acts like a reaction chamber to which more reactant molecules are being continuously added by the incoming flow. Using this concentration-enhanced enzyme assay, two cellular kinase activities (MAPKAPK2 and Protein Kinase A) were measured directly from unfractionated cell lysates yielding a sensitivity good enough to measure the activity from a few cells [16].

While the sensitivity gains in this concentration-enhanced enzyme assay are desirable, this mode raises two valid questions. First, can one still extract important reaction parameters from this experiment, since the reaction in the accumulated plug would not be directly comparable to the usual isolate chamber reaction format as both reactants would be accumulating and reacting simultaneously with a potentially continuous turnover of substrate. Second, in complex samples like cell lysates (especially in the kinase activity assay using the

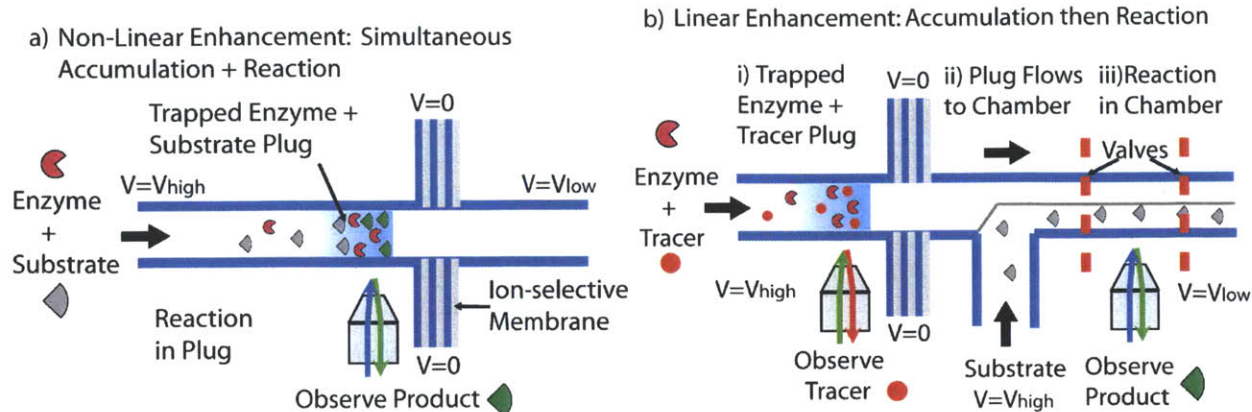


Figure 3.1 Non-linear enhancement mode of concentration-enhanced enzyme assay with simultaneous accumulation of reactants and reaction in the trapped plug **b**. Linear enhancement mode where only enzyme is accumulated into a plug and then mixed with a fixed amount of substrate in an integrated chamber where reaction occurs.

chemosensor Sox-substrates [17]) would there be interference or non-specific reaction between the fluorogenic substrate and non-target kinases, especially when the substrate might possibly get accumulated to higher levels than starting conditions. These questions necessitate a careful characterization to understand the differences between standard equilibrium reaction kinetics and concentration-enhanced enzyme reaction kinetics.

In this work we first study this unique concentration-enhanced reaction kinetic regime, which results in a non-linear enhancement of product formation rate. We develop a simple model for the reaction kinetics in the plug based on a modification of the standard Michaelis-Menten model and present an experimental verification of our model using a concentration-enhanced reaction of the widely used reporter enzyme β -Galactosidase with a fluorogenic substrate. We show that while the product formation rate is non-linear in time, a linear calibration curve from initial reaction rate to enzyme concentration is in fact expected and is experimentally obtained. This mode of enhancement is thus suitable for detecting very low activity levels with maximum amplification.

We also then propose and demonstrate a new scheme (depicted in Figure 3.1b) which linearly enhances the enzymatic reaction rate by accumulating only the enzyme molecules and mixing the concentrated enzyme plug with a fixed amount of substrate and placing and observing the reaction mixture in a closed picoliter-scale reaction chamber on chip. We demonstrate that reaction kinetics in this scheme obeys the standard Michaelis-Menten model while still benefitting from the increased enzyme concentration. This mode of enhancement is suitable for mechanistic studies with low abundance enzymes such as cellular kinases as well as for applications such as studies of inhibitory action of drugs on them where fixed amounts of other agents can be introduced via the substrate inputs into the reaction chamber.

3.2 Experimental Methods

Device Fabrication

The integrated concentrator and reaction chamber device was fabricated using a standard two layer soft lithography protocol for making the PDMS channels and valves and a Nafion surface-patterning and sealing method reported earlier [14] for making the concentrator membrane. These processes are described here in brief for completeness. A 10 μ m tall AZ4620 positive photoresist was patterned on a 6 inch silicon wafer to make the mold for the flow layer of the PDMS device. This photoresist layer was reflowed for 30 minutes at 150C to yield rounded channels. A 15 μ m tall SU-8 (SU-8 2015, Microchem Inc, Newton, MA) mold was made on another 6 inch silicon wafer for the pneumatic valve control layer of the device. Both the masters were silanized by placing them inside dessicators with a drop each of Heptadecafluoro-1,1,2,2-tetra- hydrodecyl trimethoxysilane (Gelest Inc, Morrisville, PA) and venting the

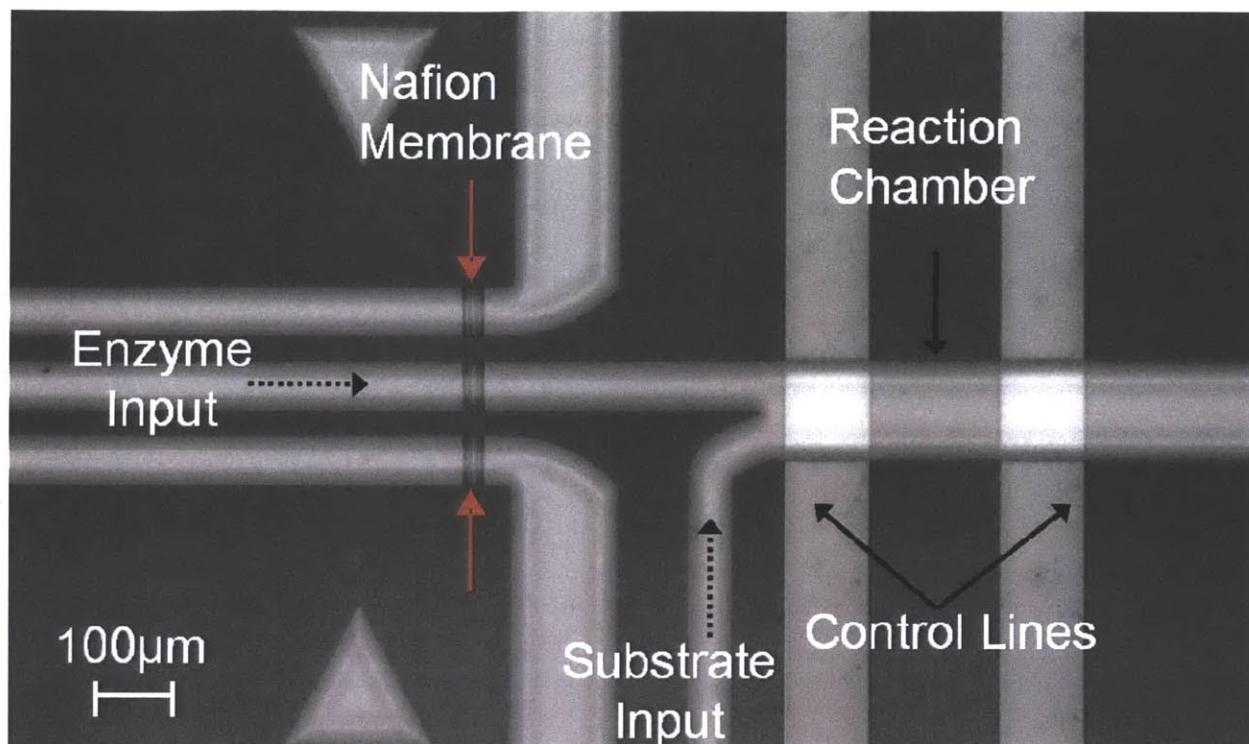


Figure 3.2 Micrograph of fabricated concentration-enhanced enzyme assay device which is used to implement both non-linear and linear enhancement mode experiments [18].

dessicators for 1 minute and maintaining the vacuum for 1 hour. A thin layer of mixed and degassed PDMS (Dow Corning Inc, Midland, MI, Sylgard 184, 20:1) was spin-coated at 2500RPM on the flow-layer mold. A thicker layer of PDMS with a higher amount of curing agent (5:1) was poured on the valve-layer mold. Both PDMS layers were partially cured for 30 minutes at 65C. The thicker valve-layer PDMS was then peeled from its mold and aligned to the flow layer on its mold under a microscope and brought into contact with it. After ensuring proper bubble-free contact, the mold was further cured overnight at 65C to obtain monolithic devices. The Nafion membrane was cast using a PDMS piece with a 50 μ m tall and 50 μ m wide straight microchannel with access holes which was reversibly sealed to a solvent-cleaned glass piece. A 20% alcohol suspension of Nafion (Sigma Aldrich Inc) was filled into this channel by

venting one of the access holes. The casting PDMS piece was then carefully removed and the Nafion pattern was allowed to dry for 1 hour at room temperature. The cured monolithic PDMS piece with channels and valves was cut and peeled from the flow layer mold and access holes were punched into it using a biopsy punch. It was then exposed to plasma along with the glass piece bearing the patterned, dried Nafion membrane and both were aligned and brought into contact. The assembled devices were baked at 65C for atleast an hour and were degassed for 15 minutes under vacuum before use. The active area of a fabricated device is shown in Figure 3.2. Plastic pipette tips were attached to the access holes to act as reservoirs.

Materials

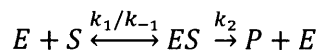
To demonstrate the use of the devices, the enzyme β -Galactosidase (from E. Coli) (β -Gal) and the fluorogenic substrates fluorescein di- β -galactopyranoside (FDG) and resorufin β -D-galactopyranoside (RDG) (all from Sigma-Aldrich Inc) were used. B-Phycoerythrin (BPE) and Alexa-488 tagged bovine serum albumin (Invitrogen Inc) were used as fluorescent tracers for enzyme accumulation. 1X PBS (pH=7.4) and magnesium chloride were obtained from Sigma-Aldrich Inc and a reaction buffer with final concentration of 10mM magnesium chloride in 0.01X PBS was prepared. Stock solutions of both enzyme and substrate were diluted before use to the concentrations needed into this buffer. A 1% w/v solution of Bovine Serum Albumin (BSA) (Sigma-Aldrich Inc) in the same buffer was used for coating the channel surfaces before the experiment to reduce non-specific binding of proteins.

Measurement

An inverted epifluorescence microscope IX71 (Olympus, Melville, NY) equipped with a LED-based light source and electronic shutter (CoolLED Ltd, UK) and a thermoelectrically cooled CCD camera (Hamamatsu Co., Japan) was used for imaging. Chroma C38229 (Fluorescein) and Omega XF108-2 (Rhodamine) filter sets were used to observed green and red fluorescence emission respectively. Open source microscopy software, μ Manager (www.micromanager.org) was used for image acquisition and NIH ImageJ was used for image analysis. Fitting and plotting was done using MS Excel and programs written in MATLAB.

3.3 Reaction Kinetics Model and Simulation

We consider an enzyme catalyzed reaction where a substrate, S is irreversibly converted to a product P in the presence of the enzyme E going through the bound intermediate state ES . With k_1, k_{-1} and k_2 as the rate constants of the reactions, this reaction can be represented as:



In order to understand the kinetics of product formation in the trapped plug in the concentrator device and to compare it with standard closed system enzyme kinetics, we make a few simplifying assumptions about the device operation. The concentrator device is assumed to be able to trap all the incoming reactant molecules into the stationary plug without any losses while letting all carrier fluid i.e. water flow past the plug without a significant change in plug volume. The trapped plug is thus assumed to act as a reactor of constant volume to which enzyme and substrate molecules are continuously added by the incoming flow from the reservoir. The plug is also assumed to act as a well-mixed reactor. Further, the reaction rate in

the input reservoir is assumed to be negligible so that the incoming reactant concentration remains constant. Note that this is expected to be valid at low enough input enzyme concentration which is the domain of application of this device.

Under these assumptions, representing the concentration of the species E by $[E]$ and so on, with $[E_0]$ and $[S_0]$ as the input concentrations of enzyme and substrate respectively in the reservoir and α as a proportionality factor representing the accumulation rate[‡], the rate equations and mass conservation for total amount of enzyme can be written as:

$$\frac{d[E]}{dt} = -k_1[E][S] + (k_{-1} + k_2)[ES] + \alpha[E_0] \quad (1)$$

$$\frac{d[S]}{dt} = -k_1[E][S] + k_{-1}[ES] + \alpha[S_0] \quad (2)$$

$$\frac{d[ES]}{dt} = k_1[E][S] - (k_{-1} + k_2)[ES] \quad (3)$$

$$\frac{d[P]}{dt} = k_2[ES] \quad (4)$$

$$[E_T] = [E_0](1 + \alpha t) = [E] + [ES] \quad (5)$$

Here the terms that appear due to the accumulation into the plug are highlighted in bold font. We explore this model first by simplifying arguments to obtain the initial and final rates and then by numerical simulations to obtain the complete product formation curve.

For $\alpha = 0$, the above set of equations reduce to the standard model of enzyme kinetics in a closed system[19]. As proposed by Briggs and Haldane[19], the enzyme-substrate binding step can be assumed to be quick and bound intermediate can be assumed to quickly reach a quasi-steady state ($d[ES]/dt \sim 0$). So, the initial product formation rate can be expressed in the standard Michaelis-Menten form:

$$\left. \frac{d[P]}{dt} \right|_{t=0} = k_2[E_0] \cdot \frac{[S_0]}{\frac{k_{-1}+k_2}{k_1}+[S_0]} = v_{MAX} \cdot \frac{[S_0]}{K_M+[S_0]} \quad (6)$$

using (3) and (4) where K_M and v_{MAX} are the Michaelis constant and the maximum reaction velocity respectively.

With non-zero accumulation rate α , we can similarly estimate the initial rate by assuming that enzyme-substrate binding is quick relative to the accumulation. Also, the usual high initial substrate concentration ($[S_0] \gg [E_0]$) results in a proportionally high substrate accumulation rate which is expected to result in a quick rise of substrate concentration in the plug initially. So, although free enzyme is continuously added to the plug from the reservoir by the flow, almost all enzyme can be assumed to quickly bind with excess substrate in the plug and end up in the bound intermediate state as soon it arrives in the plug. Thus, in the plug:

$$[E] \sim 0 \Rightarrow [ES] \sim [E_T] = [E_0](1 + \alpha t) \quad (7)$$

Then using (4):

$$\left. \frac{d[P]}{dt} \right|_{t=0} \sim k_2[E_0](1 + \alpha t) = v_{MAX}(1 + \alpha t) \quad (8)$$

Integrating this:

$$[P] \sim [P_0] + v_{MAX}t + \frac{1}{2}\alpha v_{MAX}t^2 \quad (9)$$

Thus, initially the product formation curve is expected to have a quadratic shape. In this initial phase, the rate of reaction is limited by the arrival rate of the free enzyme and we call this an *enzyme-limited* phase. In this phase:

$$\left. \frac{d[P]}{dt} \right|_{t=0} \sim v_{MAX} \quad \& \quad \left. \frac{d^2[P]}{dt^2} \right|_{t=0} \sim \alpha v_{MAX} \quad (10)$$

Note from (8) and (10) that in this phase the product formation rate is independent of substrate concentration but is linear in enzyme concentration with a slope which increases with the time. This is expected to make the device operating in this mode effective in detecting very low enzyme activities by using this amplification with time.

At later times as the enzyme molecules recycle while the substrate is irreversibly converted to product, an eventual excess of enzyme is expected to build up in the plug and all arriving substrate molecules quickly bind to excess enzyme as they arrive in the plug. So in this *substrate-limited* phase:

$$\frac{d[S]}{dt} \sim 0, \frac{d[ES]}{dt} \sim 0 \quad (11)$$

Using (11) along with (1)-(5):

$$\frac{d[P]}{dt} |_{t \rightarrow \infty} \sim \alpha[S_0] \quad (12)$$

This implies that at later times a linear product formation curve is expected.

We verify the validity these simplifications by numerically solving the system (1)-(5) of ordinary differential equations. Here, we integrated them as an initial value problem in MATLAB using the Runge-Kutta-(4,5) solver ode45. The results of these simulations for no accumulation, $\alpha [s^{-1}] = 0$ (with reaction parameters $k_1[\mu M^{-1}s^{-1}] = k_{-1}[s^{-1}] = 0.01$, $k_2[s^{-1}] = 1$) and initial values $[S_0] = 20\mu M$ and $[E_0] = 0.01\mu M, 0.1\mu M$, which are experimentally reasonable starting conditions are shown in (red and magenta) product curves in Figure 3.3a. The effect of initial enzyme concentration can be seen in this plot as at low enzyme concentration, product curve $[P2]$ rises slow and remains linear within the simulation time

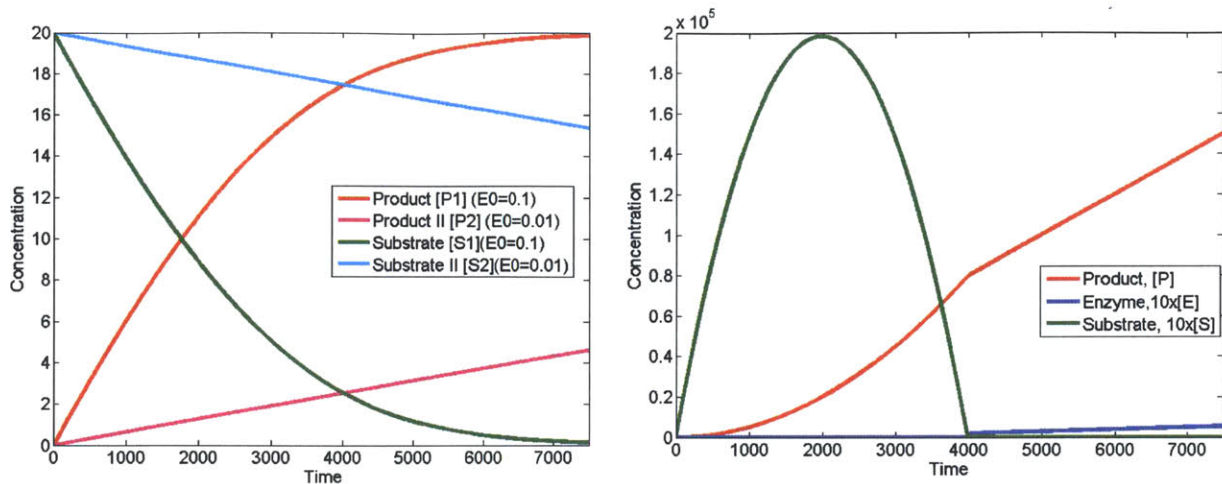


Figure 3.3 a. Numerical simulation results for an enzyme-substrate reaction modeled in the system of equations (1)-(5) with *no accumulation* i.e. $\alpha = 0$, with parameter values $k_1 = k_{-1} = 0.01$ and $k_2 = 1$ and initial values $[E_0] = 0.01, 0.1$ and $[S_0] = 20$ **b.** Enzyme-substrate reaction in the trapped plug with a *constant accumulation rate*, $\alpha = 1$ due to fluid bringing adding unreacted enzyme and substrate – with same parameter and initial values. Note that in this case, for easier visualization enzyme and substrate concentrations are scaled 10-fold and plotted [18].

window while at the higher enzyme concentration, product curve $[P1]$ rises faster and levels off due to substrate depletion.

With accumulation, setting $\alpha = 1^{\ddagger}$, the results for the same initial conditions and reaction parameters as above are shown in Figure 3.3b. Note from the different y-axis scale that the reaction product concentration rises much faster in this case. Also the (red) product curve clearly shows the quadratic and linear phases as argued above. Further, the initial high substrate concentration in the enzyme-limited phase and the later higher enzyme concentration in the substrate-limited phase can be clearly observed in the (blue) enzyme and (green) substrate concentration curves respectively. (See Supplementary Figure 1 for further simulated curves at different initial substrate concentrations). This simulation result clearly agrees in expected shape – with an initial quadratic and later linear phase – with the analytical approximations made earlier. This further justifies our earlier simplifying assumptions and in

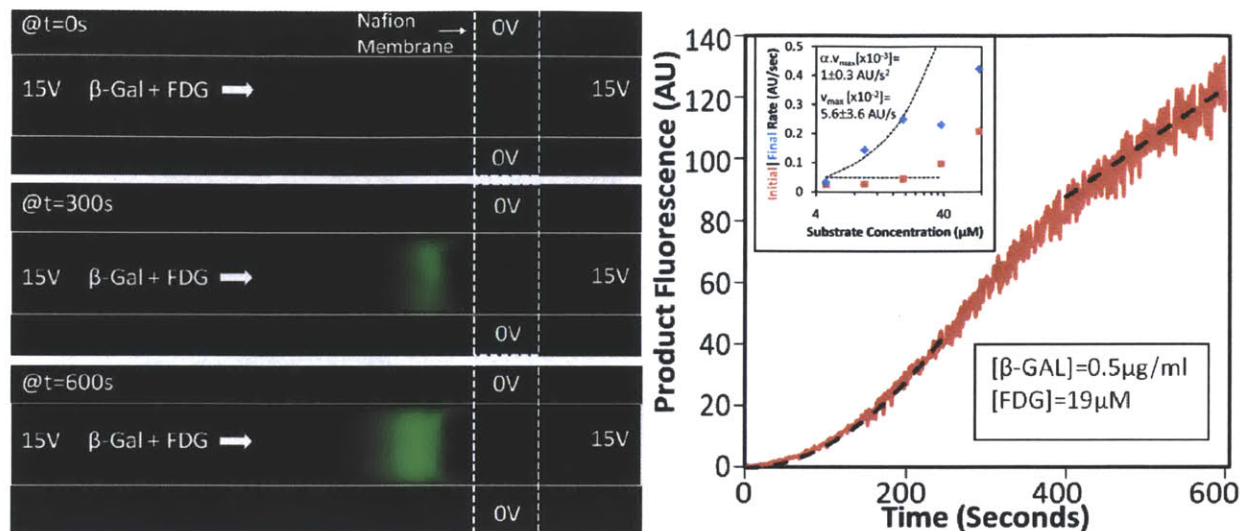


Figure 3.4 a. Fluorescence micrographs of trapped reaction plug at different time intervals after starting the reaction and accumulation. **b.** Variation of the mean fluorescence of the plug with time. The two black dotted lines are quadratic and linear fits to the segments of data on which they are shown. The inset shows the variation of initial and final reaction rates with substrate concentration [18].

fitting the experimental data we use the initial and final rate expressions (10) and (12) derived above.

3.4 Non-linear Enhancement Mode Experiments

Non-linear enhancement experiments were performed in the device shown earlier in Figure 3.2 by using only the enzyme input reservoir and channel and introducing enzyme and substrate mixed off-chip. In this experiment, the enzyme β -Galactosidase was mixed at a final concentration of $0.5\mu\text{g/ml}$ with fluorogenic substrate fluorescein di- β -galactopyranoside (FDG) and the mixture was loaded into the enzyme input reservoir and a gravity driven flow was established, controlled by a difference in fluid height between the enzyme input reservoir and the common output reservoir. A potential difference was then applied across the Nafion membrane by applying a voltage (10V-25V) to platinum electrodes dipped in the input and

output reservoirs while grounding both the adjoining buffer channels. Both β -Galactosidase (pI=5.1) [20] and FDG [21] are expected to be negatively charged at this pH and hence expected to be trapped and accumulated in the electric field gradient zone formed near the membrane. β -Galactosidase catalyses the hydrolysis of non-fluorescent FDG to form the green fluorescent product fluorescein. A green fluorescent plug formed upstream of the membrane as shown in Figure 3.4a. This region was observed at fixed intervals and the average fluorescence of the plug was measured and is plotted in Figure 3.4b.

This product curve shows an initial non-linear phase, which was found to fit well to a quadratic polynomial in time, and a later linear phase. The plot in Figure 4b also shows that the experimental product curve is in broad agreement to the model and simulation described above. The experiment was repeated with different substrate concentrations (data shown in Supplementary Figure 2) and the variation of initial and final product formation rates is shown in inset in Figure 3.4b. Note that the final saturation phase that is expected in closed-chamber enzymatic reactions with fixed amounts of reactants, due to substrate depletion, is not observed even at long times in this case. This is because unconverted substrate is continuously flowed in from the reservoir which gets added to and converted in the plug without significantly diluting the existing enzyme concentration in the plug. This feature results in a continuously rising, very high amount of product fluorescence from the trapped enzyme which can be very useful in studies from very small amounts of enzyme such as from a single or few cells. The final limit on this continuous amplification may appear due to effects such as product inhibition that occur at very high product concentrations.

To further verify our understanding of the kinetics and the applicability of the asymptotic analytical model proposed for the initial enzyme-limited and final substrate limited rates in equations (9) and (12) respectively, the variation of these rates was studied with varying initial substrate concentration. As seen in the inset in Figure 3.4b, for a range of substrate concentrations ($[S_0]=4.75\mu\text{M}$ to $38\mu\text{M}$), the initial rate (0-10s) remains independent of substrate concentration as predicted by equation (10) while the final rate (550-600s) increases linearly with substrate concentration as predicted by equation (12). Quadratic polynomials in time were fitted to the initial non-linear phases (0-200s) of the product curves at different substrate concentrations and these were found to have constant curvatures as predicted by equation (10). These polynomial fits (along with a fluorescence (AU) to product concentration (μM) calibration shown in Supplementary Figure 3) were used to obtain the value of the parameters $\alpha v_{MAX}=1.0 \pm 0.3 \times 10^{-3} \text{AU}/\text{s}^2 = 4.6 \pm 1.4 \mu\text{M}/\text{s}$ from the quadratic term and $v_{MAX} = 5.6 \pm 3.6 \times 10^{-2} \text{AU}/\text{s} = 21.2 \pm 16.6 \mu\text{M}/\text{s}$ from the linear term. The higher error in the linear term is possibly due to differences in starting observation times in the different reactions. Similarly the later linear phase can be used to obtain $\alpha = 6.75 \times 10^{-2}/\text{s}$. This is lower than the estimated value of $\alpha \sim 0.5$, possibly due to dispersion of molecules or a lower than estimated flow velocity due to channel height variation. This along with the earlier quadratic term then yields a lower estimate of $v_{MAX} = 1.5 \pm 0.4 \times 10^{-2} \text{AU}/\text{s} = 6.9 \pm 1.8 \times 10^{-2} \mu\text{M}/\text{s}$. At higher substrate concentrations ($[S]>38\mu\text{M}$) the product curves deviate significantly from this predicted form and become completely linear in time and the initial rates rise linearly with substrate concentration too. This could be because the assumption of very low reaction rate in input reservoir might

break down at such high substrate concentrations and there may be a significant contribution of direct accumulation of product already formed in the reservoir into the observed plug adding to or overshadowing the reaction in the plug itself. This can be compared with the product accumulation device reported recently by Cheow *et al* [22] where the reaction always happens upstream of the plug at enzyme-coupled beads and linear product accumulation curves are obtained.

An important conclusion from this model and the above observations verifying it is that the concentration-enhanced reaction in the accumulation plug ultimately enters a substrate-limited linear regime where adverse effects of excessive substrate accumulation – such as reactions with non-target kinases in cell lysates due to an uncontrolled substrate concentration are not expected to happen [16]. Also the simple model still provides an opportunity to find reaction parameters such as v_{MAX} from experimental data although within limits of relatively low substrate concentrations.

We also directly verified the linearity of initial reaction rates with enzyme concentration as predicted in equation (8). To avoid variability due to different starting observation times and other device and experimental variations, we ran five simultaneous reactions using a 5-channel multiplexed version of the device reported earlier¹². The results from this experiment are shown in Figure 3.5. The input reservoirs of the five channels are loaded with the same volume of enzyme-substrate mixtures at the same substrate concentration but differing enzyme concentrations and the same potential is applied to all the channels and the three reaction plugs are observed simultaneously as shown in Figure 3.5a. The five product curves are

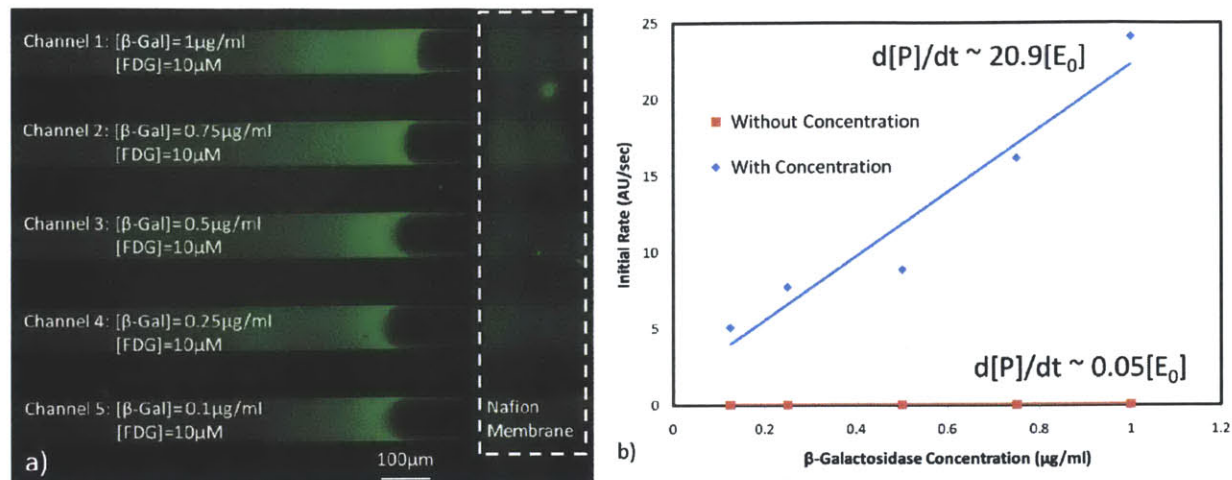


Figure 3.5 a. Five simultaneous reactions in the non-linear enhancement mode running in a multiplexed device with different enzyme concentrations. **b.** Initial reaction rates versus enzyme concentration show that the rate rises linearly with enzyme concentration. The initial rate is enhanced $\sim 400\text{X}$ at all the five enzyme concentrations when the potential is applied to accumulate the reactants and the product [18].

analyzed as earlier and the initial rates of product formation with and without application of the trapping voltage are plotted in Figure 3.5b. A 400-fold enhancement in reaction rate is observed while linearity with enzyme concentration is maintained.

3.5 Linear Enhancement Mode Experiments

To demonstrate the proposed linear enhancement mode, the enzyme and substrate solutions were loaded into separate input reservoirs attached to the two input channels of the device shown in Figure 3.2. Only the enzyme would be accumulated into a plug in this case so the enzyme solution was spiked with a fluorescent tracer to make the plug visible. These experiments were performed with two different substrates: Fluorescein β -D-galactopyranoside (FDG) as described above and Resorufin β -D-galactopyranoside (RDG) which gets hydrolysed to red fluorescent product Resorufin. The tracer was chosen to have a different emission color than the fluorescent reaction product to avoid interference with later observation of the reaction

progress. A red fluorescent protein, β -Phycoerythrin was used as tracer for the FDG reaction while a green fluorescent protein, Alexa[®] 488 tagged BSA was used as a tracer in the RDG reaction. Gravity-driven flows of enzyme and substrate were established in the device with identical pressure heads and the mixing of the two reactant streams could be observed in the reaction chamber both in the tracer fluorescence and in the fluorescence of the product as it formed at the mixing interface. As a control experiment without accumulation of the enzyme, the valves were closed in this condition by applying and holding air pressure using tubing attached to a syringe and the reaction was observed in the closed chamber using the product fluorescence filter set.

For observing the reaction with accumulation of the enzyme – a potential difference was applied across the Nafion membrane as earlier. To maintain identical flow of enzyme and substrate, the same voltage was also applied to the substrate input reservoir. During the accumulation, the region upstream of the membrane was observed using the tracer fluorescence filter set. A tracer plug formed near the membrane (Figure 3.6a.i) and it grew in brightness over time as more of the tracer accumulated in the plug. After 20 minutes of accumulation, the plug was released by turning the voltage off and it was pushed downstream by the flow (Figure 3.6a.ii). The plug met the substrate flow at the junction and moved into the reaction chamber region. When the plug was positioned in the reaction chamber, the valves were closed (Figure 3.6a.iii) and the image acquisition was started under the product filter set with the same exposure time and frame rate as in the control experiment. The time variation of product

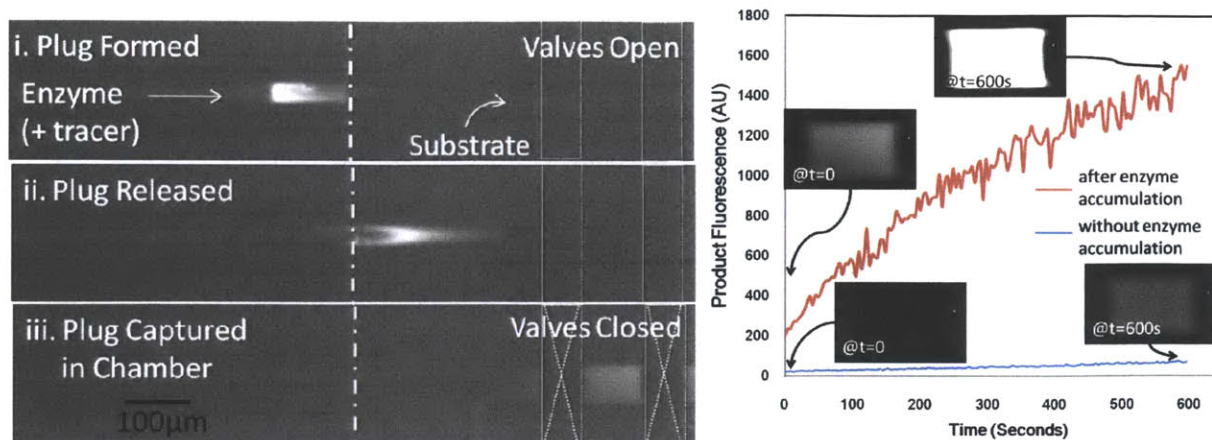


Figure 3.6a Fluorescence micrographs showing the operation of the device **i**. The tracer protein, B-Phycoerythrin is concentrated into a plug by applying the voltage **ii**. The plug released by turning the voltage off and is driven by gravity driven flow to the reaction chamber. **iii**. The pneumatic valves are actuated to capture the plug **b**. Variation of peak green fluorescence in the reaction chamber with time for the reaction between β -Galactosidase and FDG with and without accumulation of the enzyme. The insets show the reaction chamber at the beginning and end of the observation period [18].

fluorescence in the chamber is plotted in Figure 3.6b along with that from the control experiment. We assume here that the enzyme plug is formed at the same position as the tracer plug and hence gets transferred to chamber along with it. This was experimentally verified by changing the position of the tracer plug relative to the valves before closing them and it was observed that the maximum reaction rate was obtained when the tracer plug was centered in the chamber. A 50-fold increase in the initial product formation rate is observed due to the increased enzyme concentration from the trapped plug. The control experiment has a very low amount of enzyme present in the chamber and hence the product curve obtained remains in the initial linear region (as predicted in simulated product curve [P2] in Figure 3.3a) till the end of the 10 minute observation period. However with the accumulated enzyme plug, the product curve shows the effect of higher enzyme concentration and we observe substrate depletion and

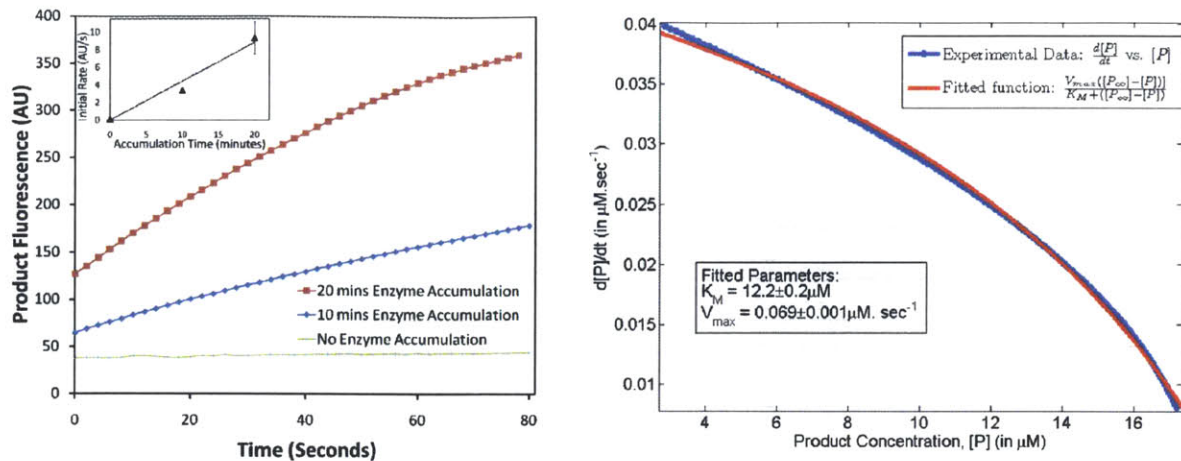


Figure 3.7a Variation of peak red fluorescence in the reaction chamber with time for the reaction between the enzyme β -Galactosidase and RDG with different accumulation times of the enzyme. **b.** Variation of product formation rate in the linear enhancement mode as measured by the rate of variation of mean fluorescence in the closed chamber and a fitting of the expected Michaelis-Menten form to the experimental data in order to obtain reaction parameters [18].

the resultant reduction in reaction rate with time (as predicted in simulated curve [P1] in Figure 3.3b). In this mode product curves are found to fit the standard Michaelis-Menten kinetics model (as shown in Figure 3.7b) as derived in equation (6) from which the parameter K_M was extracted as $\sim 12\mu\text{M}$ and $v_{MAX} \sim 6.9 \times 10^{-2} \mu\text{M}/\text{s}$ which is within the range of reported values [23].

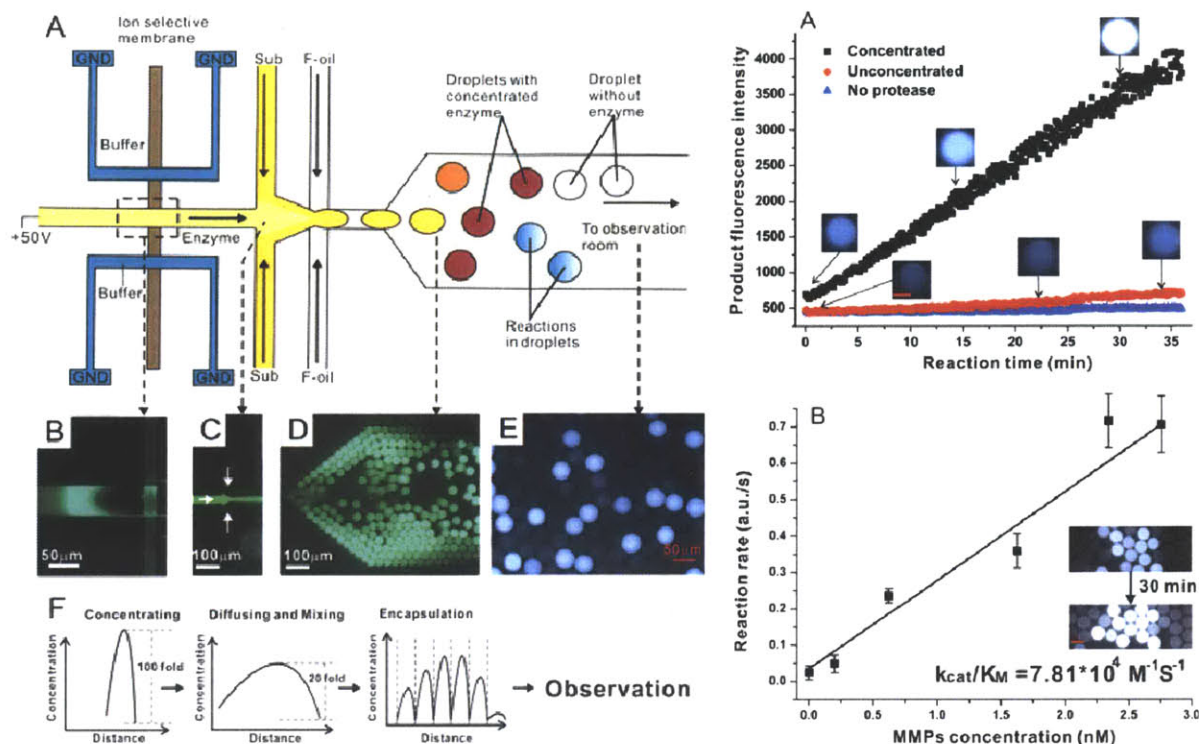
The enzyme concentration in the captured plug and hence the level of enhancement of the reaction rate can be tuned by changing the time for which the enzyme is accumulated before releasing it into the reaction chamber. The effect of accumulation time on the reaction rate is shown in Figure 3.7a. Longer accumulation times yield higher reaction rates in the chamber due to higher concentration of enzyme in the incoming plug. The reaction rates variation with enzyme accumulation time is shown in the inset in Figure 6c. Each data point here indicates the mean and standard deviation from three experiments. A 73-fold enhancement of reaction rate is

obtained for 20 minutes of enzyme accumulation time. For a given accumulation time, the product curve obtained is repeatable over experiments as evidenced in the small variation in initial rates measured over three experiments.

A current limitation of this device in this mode is the reduction in enhancement due to the dispersion during transfer from the concentrator region to the reaction chamber which is evident in the tracer plugs seen in Figure 3.6a. The dispersion is expected to decrease with the distance between these regions which is dependent on the alignment accuracy between the two-layers of PDMS during device fabrication which can be reduced by optimizing the fabrication process further.

3.6 Integration with Droplet-Based Microfluidics

Droplet-based microfluidics affords the ability to run massively parallel reactions in thousands of droplets [24, 25] which is desirable in order to monitor the enzymatic activity of physiological samples using extremely small amounts of sample and reagents. However, the analysis of low-abundance enzymes directly from physiological samples in droplets is challenging because of the low assay sensitivity, the long assay times and the nonspecific loss of target biomolecules to droplet interfaces. Random encapsulation of individual biomolecules into droplets could increase the effective concentration within droplets and enhance the assay sensitivity [26]. However this mode of enhancement is limited because even in the smallest stable droplets (diameter $\sim 5 \text{ }\mu\text{m}$), a single trapped molecule is equivalent to an effective concentration of $\sim 1\text{pM}$, which is still below the detection limit of many conventional assays, such as capillary electrophoresis-based assays and immunoassays. So far, methods for controlling



reactant concentrations in droplets rely on further dilution of the sample to tune the ratio of the different reactants [28]. Thus, a reliable and programmable method to increase the concentration of biomolecules within droplets is required to take advantage of the full potential of droplet-based microfluidics.

Here we further implement the linear-enhancement mode of concentration-enhanced enzyme assay developed above using water-in-oil droplets as isolated reaction chambers by

integrating a biomolecule concentrator and a droplet generator in a single chip (shown in Figure 3.8a), exploiting the complementary advantages—sensitivity enhancement and effective encapsulation—of these two technologies. Additionally, the multiplexed assays can be completed with a minimal amount of sample reagent because numerous droplets that have different sample concentrations are used as individual reaction chambers. Thus, this integrated device has the ability to detect low-abundance enzymes and other relevant biomarkers in complex physiological samples with high sensitivity and throughput, and therefore can be a generic tool for systems biology research and medical diagnostics.

3.7 Measurement of Activity of Secreted Matrix Metalloproteinases

We use this integrated platform to study secreted proteases from the matrix metalloproteinase family which participate in diverse biological and pathological processes [29]. As the key degradative enzymes of the extracellular matrix, MMPs play a critical role in cancer development and metastasis [30]. Existing enzyme activity assays either lack the sensitivity required to directly detect the protease activity in limited sample quantities or suffer from low throughput [14]. We first employed our platform to study the activity of a recombinant matrix metalloproteinase (MMP-9, 0.2nM in MMP buffer [30]) in using a FRET-based polypeptide MMP substrate (5 μ M), which fluoresces upon cleavage as an indicator of proteolytic activity. MMP-9 activity was monitored in the individual droplets. We observed very small fluorescence changes (\sim 25a.u.) for the negative-control samples lacking protease (Figure 3.8b). For droplets containing the protease, the fluorescence intensities of the turned-over substrate increased linearly with assay time in both experiments with and without the concentration step. After the

preconcentration step, the concentration of MMP-9 in the droplets increased up to 16-fold (inferred by the tracer fluorescence) which correlated with the identical increase in activity measured using product fluorescence.

Additionally, different enzyme concentrations (from 0.2nM to 3.2nM) were screened in a single experiment to obtain information on reaction kinetics, as shown in Figure 3.8b. The concentration range could be tuned by selecting the distance. As expected, the reaction rates showed an almost linear increase with increasing MMP-9 concentration. After calibration of the fluorescence intensity of the product, the value of the kinetic constant ($k_{cat}/K_m = 7.81 \cdot 10^4 M^{-1}S^{-1}$) was obtained by assuming that Michaelis-Menten kinetics were obeyed. This result was consistent with the value obtained using a standard plate-reader and with the value from a previous study on protease activity [30].

We then performed the experiments with diluted conditioned media from in vitro tissue culture samples (0.5X cellular supernatant dilutions in MMP buffer) to study the protease activity in the media. Specifically, we examined stimulated and untreated protease activity of the culture media from mouse embryonic fibroblasts (MEF) in response to cytokine treatment. For both stimulated and untreated samples, the proteolysis reaction caused the fluorescence intensity to increase linearly over time (**Error! Reference source not found.a**). After concentrating the sample, the difference in activity between the stimulated and untreated samples was amplified ~10-fold compared to difference between the unconcentrated samples. The detection sensitivity for the stimulated and untreated conditions was thus improved, allowing us to clearly differentiate

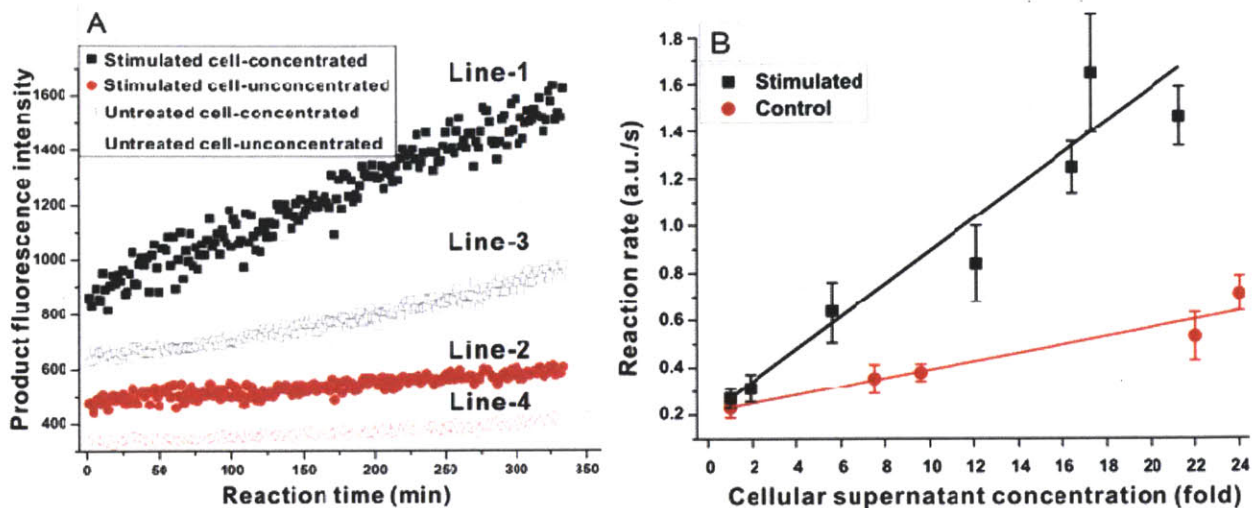


Figure 3.9a Increase in product fluorescence intensity in an individual droplet with reaction time after mixing the cellular supernatant and the sensor is shown. The reaction rates, as determined by substrate turnover resulting from proteolysis in cellular supernatant, were monitored as a function of time. The activities of the stimulated samples (concentrated and unconcentrated) are represented by line-1 and line-2, respectively. The activities of untreated samples are shown in line-3 (concentrated) and line-4 (unconcentrated). The difference in the reaction rates was greater for the concentrated samples than for the unconcentrated samples, and thus, the assay sensitivity was improved. b. The reaction rate increased with increasing cellular supernatant concentrations in the droplets. A linear relation was observed between the reaction rate and the initial concentration. Each data point represents the average of five droplets, and the error bar represents the standard deviation [27].

these conditions by the slopes of the fluorescence intensity increase over 5 min (line-1 slope: 2.14a.u./s, line-3 slope: 0.95a.u./s). In the unconcentrated assay, the traces of the stimulated condition (line-2 slope: 0.32a.u./s) were significantly different from those of the untreated condition (line-4 slope: 0.22a.u./s) only after 50 min of reaction time. Taking advantage of the high-throughput screening made possible by using our device (**Error! Reference source not found**.b), the reaction rates over a range of concentration enhancements were determined by a single experimental run to obtain the parameters related to the reaction kinetics (stimulated sample: $(k_{cat}/K_M)[E] = 1.61 \cdot 10^{-4} S^{-1}$; untreated sample: $(k_{cat}/K_M)[E] = 4.68 \cdot 10^{-5} S^{-1}$). This experiment

required less than 25 μ L of diluted cellular supernatant. This is a \sim 100-fold reduction in sample volume compared to conventional assays.

3.8 Conclusions and Future Directions

In summary, we have demonstrated here that the nanofluidic biomolecule concentrator can be used in multiple ways to perform enzyme assays from low volume and/or low abundance samples. The enzyme reaction kinetics in these devices was studied and was found to obey simple models within certain limits of reactant concentrations. We showed that the simultaneous accumulation and reaction mode gives a high amplification factor with a product formation curve that is initially non-linearly rising in time but is linear in enzyme concentration. Finally at long enough times, this reaction mode enters a linearly rising phase which is explained in our model as a substrate-limited phase. The substrate concentration in the accumulated plug is maintained low in this phase and this enables ruling out non-target reactions of chemosensor substrates in complex mixtures such as cell lysates which might arise due to uncontrolled substrate concentrations. This allows maintaining the performance of the assay within designed limits in terms of cross-reactivity while continuously forming a large amount of product over time with a limited amount of trapped enzyme. This mode is thus well suited for detection of very low enzyme activities where a high reaction rate enhancement is the most desirable feature. We also showed the ability to multiplex these assays in the same chip which leads to the possibility of higher throughput in concentration-enhanced assays. The new separate accumulation and reaction device – implemented by integrating the nanofluidic concentrator with a chamber isolated by pneumatic valves or with a water-in-oil droplets using

a microfluidic droplet generator – offers a linearly enhanced reaction rate with a simpler product curve that replicates the standard kinetics observed in macro-scale isolated chamber assays. It offers the opportunity to perturb this kinetics – for example by adding drugs or other inhibitor molecules to the reaction chamber – and study the mechanism of reaction of low abundance enzyme molecules while maintaining an easy comparison with data from existing non-microfluidic reaction formats. It also offers the opportunity to study more complex mixtures where addition of fixed amounts of substrate maybe critical to the assays.

We also developed and demonstrated a we developed a microfluidic platform that integrates a biomolecule concentrator and a droplet generator to detect enzyme activity with high sensitivity in a high-throughput manner. This system can be used to analyze different enzyme reactions, such as those catalyzed by reporter enzymes, kinases and proteases. We specifically characterized the activity of MMPs in diluted cellular supernatant from stimulated and untreated MEF cells. The concentrator amplified the difference between the stimulated and untreated conditions and allowed a significant reduction in the reaction time (~10-fold). Moreover, the protease-substrate reaction kinetics could be determined by a parallel analysis of droplets with different amplified enzyme concentrations in a single experiment to significantly reduce the sample volume used (~100-fold). This device, with its ability to assay biochemical reactions catalyzed by low-abundance enzymes and other relevant biomarkers in physiologically complex samples, is a generic and useful platform for systems biology research and medical diagnostics.

More broadly, we have demonstrated the use of the biomolecule concentration technique as a world-chip interface which can be used to bring molecules from low concentration samples, such as from single cells, into highly concentrated very small volume plugs on chip and then manipulate and study them using flow and reaction and these platforms.

Publications and Acknowledgements

Parts of this chapter have been published before in conference proceedings and as journal articles which are listed here as references [18, 27, 31, 32]. The experiments for droplet integration and MMP assay (Figure 3.8 and Figure 3.9) were performed by Dr. Chia-Hung Chen with cellular supernatant samples provided by Mr. Miles Miller.

3.9 References

- [1] N. Kumar, *et al.*, "Quantitative analysis of Akt phosphorylation and activity in response to EGF and insulin treatment," *Biochemical and Biophysical Research Communications*, vol. 354, pp. 14-20, 2007.
- [2] S. L. Spencer, *et al.*, "Non-genetic origins of cell-to-cell variability in TRAIL-induced apoptosis," *Nature*, vol. 459, pp. 428-432, 2009.
- [3] M. Niepel, *et al.*, "Non-genetic cell-to-cell variability and the consequences for pharmacology," *Current Opinion in Chemical Biology*, vol. 13, pp. 556-561, 2009.
- [4] J. G. Albeck, *et al.*, "Collecting and organizing systematic sets of protein data," *Nature Reviews Molecular Cell Biology*, vol. 7, pp. 803-812, Nov 2006.
- [5] M. Miyazaki and H. Maeda, "Microchannel enzyme reactors and their applications for processing," *Trends in Biotechnology*, vol. 24, pp. 463-470, 2006.
- [6] W. D. Ristenpart, *et al.*, "Enzymatic Reactions in Microfluidic Devices: Michaelis-Menten Kinetics," *Analytical Chemistry*, vol. 80, pp. 3270-3276, 2008.
- [7] A. G. Hadd, *et al.*, "Microchip Device for Performing Enzyme Assays," *Analytical Chemistry* vol. 69, pp. 3407-3412, 1997.
- [8] S. Jambovane, *et al.*, "Determination of Kinetic Parameters, Km and kcat, with a Single Experiment on a Chip," *Analytical Chemistry*, vol. 81, pp. 3239-3245, 2009.
- [9] H. Song, *et al.*, "Reactions in droplets in microfluidic channels," *Angewandte Chemie-International Edition*, vol. 45, pp. 7336-7356, 2006.
- [10] G. H. S. Seong, *et al.*, "Measurement of Enzyme Kinetics Using a Continuous-Flow Microfluidic System," *Analytical Chemistry* vol. 75, pp. 3161-3167, 2003.

- [11] A. J. Hughes and A. E. Herr, "Quantitative Enzyme Activity Determination with Zeptomole Sensitivity by Microfluidic Gradient-Gel Zymography," *Analytical Chemistry*, vol. 82, pp. 3803-3811.
- [12] Y.-C. Wang, *et al.*, "Million-fold Preconcentration of Proteins and Peptides by Nanofluidic Filter," *Analytical Chemistry*, vol. 77, pp. 4293-4299, 2005.
- [13] S. J. Kim, *et al.*, "Nanofluidic concentration devices for biomolecules utilizing ion concentration polarization: theory, fabrication, and application," *Chemical Society Reviews*, vol. 39, pp. 912-922, 2010.
- [14] J. H. Lee, *et al.*, "Increase of Reaction Rate and Sensitivity of Low-Abundance Enzyme Assay using Micro/Nanofluidic Preconcentration Chip," *Analytical Chemistry*, vol. 80 pp. 3198-3204, 2008.
- [15] Y.-C. Wang and J. Han, "Pre-binding dynamic range and sensitivity enhancement for immuno-sensors using nanofluidic preconcentrator," *Lab on a Chip*, vol. 8, pp. 392-394, 2008.
- [16] J. H. Lee, *et al.*, "Microfluidic Concentration-Enhanced Cellular Kinase Activity Assay," *Journal of the American Chemical Society*, vol. 131, pp. 10340-10341, 2009.
- [17] M. D. Shults, *et al.*, "A multiplexed homogeneous fluorescence-based assay for protein kinase activity in cell lysates," *Nature Methods*, vol. 2, pp. 277-283, 2005.
- [18] A. Sarkar and J. Han, "Non-linear and linear enhancement of enzymatic reaction kinetics using a biomolecule concentrator," *Lab Chip*, vol. 11, pp. 2569-76, Aug 7 2011.
- [19] G. E. Briggs and J. B. Haldane, "A Note on the Kinetics of Enzyme Action," *Biochemical Journal*, vol. 19, pp. 338-9, 1925.
- [20] P. G. Righetti, *et al.*, "Isoelectric points and molecular weights of proteins : A new table," *Journal of Chromatography A*, vol. 220, pp. 115-194, 1981.
- [21] M. M. Martin and L. Lindqvist, "The pH dependence of fluorescein fluorescence," *Journal of Luminescence*, vol. 10, pp. 381-390, 1975/8//.
- [22] L. F. Cheow, *et al.*, "Increase of Sensitivity of ELISA using Multiplexed Electrokinetic Preconcentrator," *Analytical Chemistry*, vol. 82, pp. 3383-3388, 2010.
- [23] J. Hofmann and M. Sernetz, "A kinetic study on the enzymatic hydrolysis of fluoresceindiacetate and fluorescein-di-[beta]-galactopyranoside," *Analytical Biochemistry*, vol. 131, pp. 180-186, 1983.
- [24] A. B. Theberge, *et al.*, "Microdroplets in microfluidics: an evolving platform for discoveries in chemistry and biology," *Angew Chem Int Ed Engl*, vol. 49, pp. 5846-68, Aug 9 2010.
- [25] H. Song, *et al.*, "Reactions in droplets in microfluidic channels," *Angew Chem Int Ed Engl*, vol. 45, pp. 7336-56, Nov 13 2006.
- [26] B. Rotman, "Measurement of activity of single molecules of beta-D-galactosidase," *Proc Natl Acad Sci U S A*, vol. 47, pp. 1981-91, Dec 15 1961.
- [27] C. H. Chen, *et al.*, "Enhancing protease activity assay in droplet-based microfluidics using a biomolecule concentrator," *J Am Chem Soc*, vol. 133, pp. 10368-71, Jul 13 2011.

- [28] S. Jambovane, *et al.*, "Creation of stepwise concentration gradient in picoliter droplets for parallel reactions of matrix metalloproteinase II and IX," *Anal Chem*, vol. 83, pp. 3358-64, May 1 2011.
- [29] K. Wolf, *et al.*, "Multi-step pericellular proteolysis controls the transition from individual to collective cancer cell invasion," *Nat Cell Biol*, vol. 9, pp. 893-904, Aug 2007.
- [30] M. A. Miller, *et al.*, "Proteolytic Activity Matrix Analysis (PrAMA) for simultaneous determination of multiple protease activities," *Integr Biol (Camb)*, vol. 3, pp. 422-38, Apr 2011.
- [31] Y.-A. Song, *et al.*, "Encapsulation of Biomolecules with Programmable Concentrations in Microdroplets using Electrokinetic Concentrator," in *MicroTAS 2008*, San Diego, CA, 2008, pp. 1420-1422.
- [32] C. H. Chen, *et al.*, "Enhancing/Multiplexing Protease Assay with Droplet Based Microfluidics using Biomolecule Concentrator," in *15th International Conference on Miniaturized Systems for Chemistry and Life Sciences (μ TAS 2011)*, Seattle, Washington, USA, 2011, pp. 2080-2082.

Chapter 4 An Integrated Microfluidic Probe for Single Cell Kinase Activity Measurement

4.1 Introduction

Understanding how a cell processes information presented by external cues, through the action of internal signaling molecules, to generate a phenotypic response is essential to elucidating basic cell biology as well as for understanding and finding therapies for disease states such as cancer which result in many cases from aberrations in this signaling network. Measurement of the cellular signaling state under conditions of controlled cues and correlating it with associated cellular behavior can play an instrumental role in this pursuit. Protein kinases, which generate or relay signals by the phosphorylation of specific target molecules, form a significant fraction of the nodes in the cellular signaling network and the measurement of cellular kinase activity is thus an important tool in basic biology as well as disease research.

Most kinase activity measurement methods – like indeed most cellular biochemical assays – measure ensemble averages of large numbers (10^3 - 10^6) of cells, usually due to very low abundance of these molecules in single cells and the limited sensitivity of the detection methods. However it is increasingly obvious that cell populations are heterogeneous and such bulk measurements result in a ‘blurred’ picture of cellular signaling [1]. This may not represent the signaling state of single cells which may behave differently due to their inherent differences [2, 3] or in response to variation in their local extracellular microenvironment [4] and may in fact

control phenotypic outcomes in various life and disease processes. Measuring single cell kinase activity and correlating it to the phenotype and local extracellular context from the same single cell can thus be of great advantage in understanding cellular behavior.

Many existing single cell kinase assays, based on flow cytometry or imaging, depend on the use of phospho-specific antibodies [5] to measure the phosphorylation state of proteins as a surrogate for their activity – a correlation which may not hold true [6]. In addition, flow cytometry based methods work with cell suspensions which makes it difficult to correlate phenotype or cellular microenvironment to kinase activity for adherent cells which includes most cancer cell types except for those of hematologic or immunologic origin. Genetically encoded reporters can be used to measure protein levels, localization or activity directly [7] in live single adherent or suspended cells but require genetic manipulation of cells which may affect the system under study. Also such reporters are difficult to multiplex which limits their use. Single cell kinase activity measurement by microinjection of substrates into adherent cells has been demonstrated but can suffer from non-specific intracellular reactions [8, 9].

Direct measurement of kinase activity from single cells remains difficult, in general, due to limited assay sensitivity and the difficulty of interfacing activity measurement methods with phenotype measurement. Selective, fluorogenic peptide probes for measuring kinase activity directly in cellular media and unfractionated cell lysate have been developed [10] and have been used to probe kinase activity in bulk cell and tissue lysates [11]. Our group has earlier demonstrated the measurement of kinase activity from small amounts of bulk cell lysate (~4-5ng=4-5cells) in microfluidic chip using a biomolecular concentrator [12].

Microfluidic systems can boost assay sensitivity by scaling assay volume down. However most existing microfluidic cell analysis [13] or manipulation techniques usually work with cell suspensions which are easy to flow into microfluidic channels. Here we intend to develop an integrated microfluidic device that can interface directly with selected single, adherent cells on standard tissue culture platforms and capture their contents into a small volume and perform kinase activity measurements. This would enable the measurement of potentially complex adherent cell phenotypes such as cell migration or morphology and their correlation with kinase activity in specific single cells.

4.2 Selective Single Cell Lysis

Juncker *et al.* [14] have developed a multi-purpose, vertical, silicon microfluidic probe which is essentially a scanned probe with microfluidic channels that are used to create a small zone of a specific liquid under its tip while the probe itself can be mobile inside an open liquid environment. This is enabled by hydrodynamic confinement of the liquid from the probe using simultaneous out-flow and in-flow from ends of the microchannel at the tip at a fast enough velocity to beat diffusive mixing Figure 4.1a. This has been used for protein patterning or localized staining of cells in a tissue culture plate [14] and recently even on tissue slices [15]. It has also been adapted to a slanted probe format, fabricated in PDMS, for stimulation of single cells [16] for electrophysiological measurements which allows easier positioning and landing near cells.

Here we adapt the microfluidic probe for selective single cell lysis by flowing a scaling it

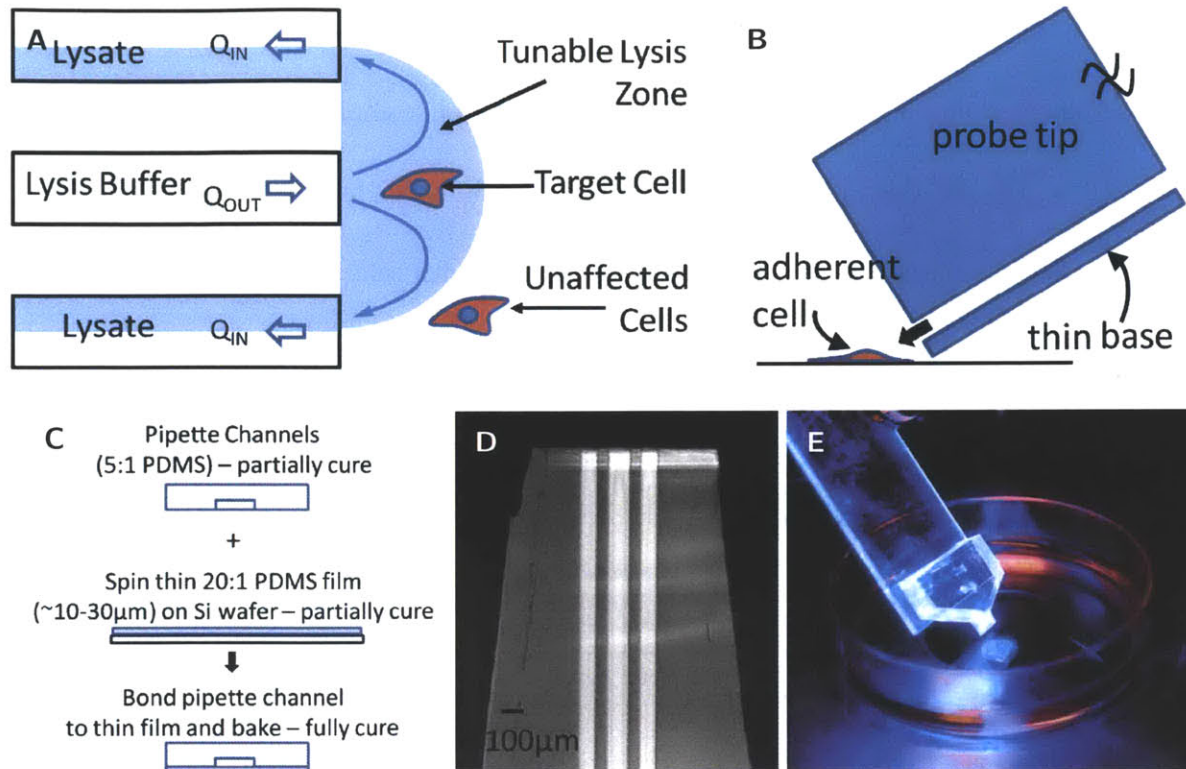


Figure 4.1a. A tunable lysis zone is formed by simultaneous in and out flow of lysis buffer established using microchannels which results in a hydrodynamically confined, small, tunable lysis zone which can be used to target single cells. **b.** The probe tip places the microchannels close to cells by having a thin membrane base **c.** This is fabricated using spin-coating and thermal bonding of a thin PDMS membrane. **D.**

down in size to target single adherent cells and flowing a detergent-containing lysis buffer in it to form a small, tunable ‘lysis zone’ at its tip. One of the key requirements for the probe tip is that it has to bring the microchannels for lysis buffer out-flow and lysate in-flow as close to single cells as possible Figure 4.1b. This was achieved by using a thin spin-coated and thermally bonded PDMS membrane as the base for the probe Figure 4.1c. The fabricated probe as shown in Figure 4.1d was mounted on a micro-manipulator which enabled dipping it into a tissue culture plate containing tissue culture medium placed on a motorized microscope stage and accurate positioning next to selected single cells which could be selected based on unique phenotypic measures demonstrated by them in a microscopy-based assay.

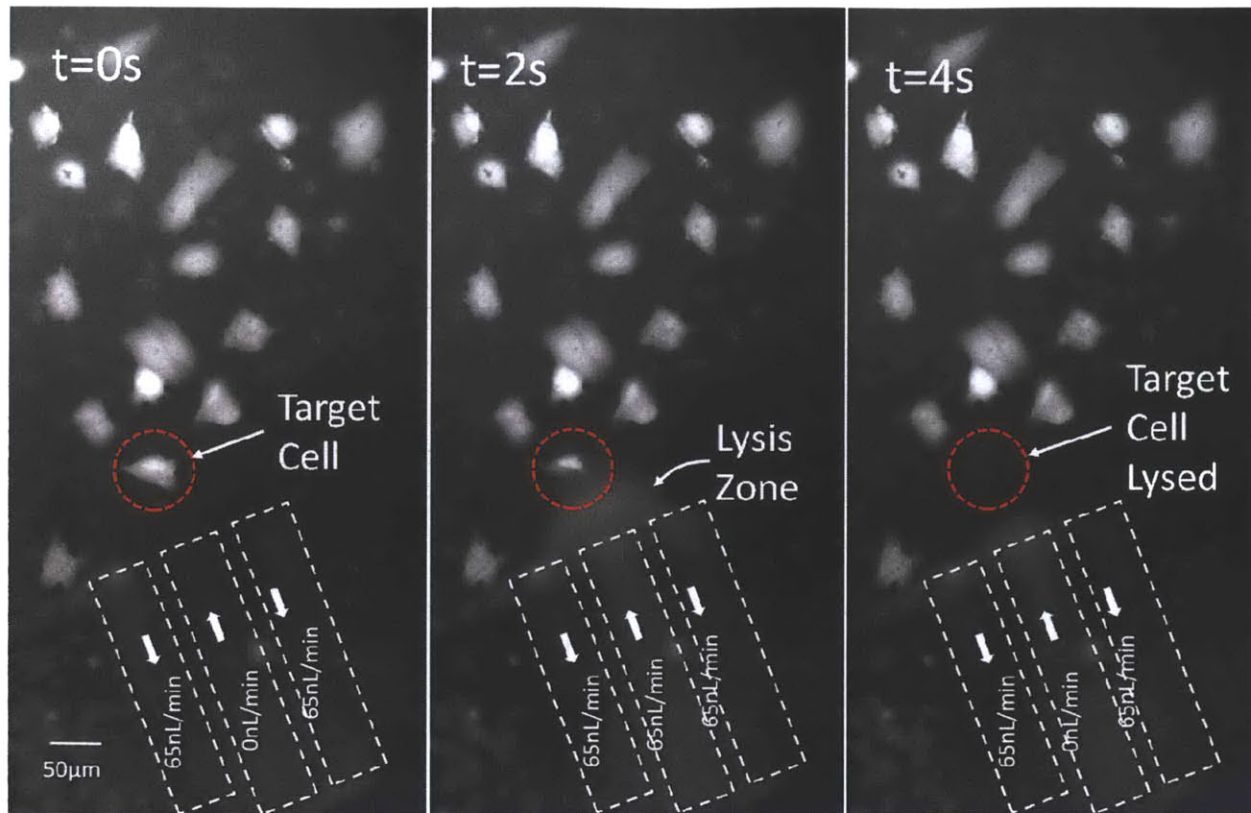


Figure 4.2 A selected cell from a green-fluorescent protein expressing adherent MCF-7 population is lysed using the microfluidic probe with a lysis buffer containing 1% Triton-X 100 while the surrounding cells remain unaffected by this process. The lysis zone can be seen in fluorescence from a tracer added to the lysis buffer.

Selective single cell lysis using this technique was demonstrated with cells expressing a fluorescent protein (MCF-7 cells, expressing GFP) as shown in Figure 4.2. The out-flow channel and in-flow channels of the probe are primed with lysis buffer containing 1% Triton-X 100 as a lysis agent (1X lysis buffer as in [17]) any assay buffer (1X assay buffer as in [17]) respectively by connecting the respective ports to 50 μ L Hamilton gas-tight syringes carrying those fluids, which are then coupled to separate Harvard Apparatus PHD 2000 syringe pumps. The probe is positioned next to a single cell and then the in-flow is established at a flow rate of \sim 130nL/min using and then a pulse (\sim 10s-60s tuned by observation) of out-flow of the lysis buffer is generated which forms a lysis zone, visualized here using a fluorescent dye added to it, which

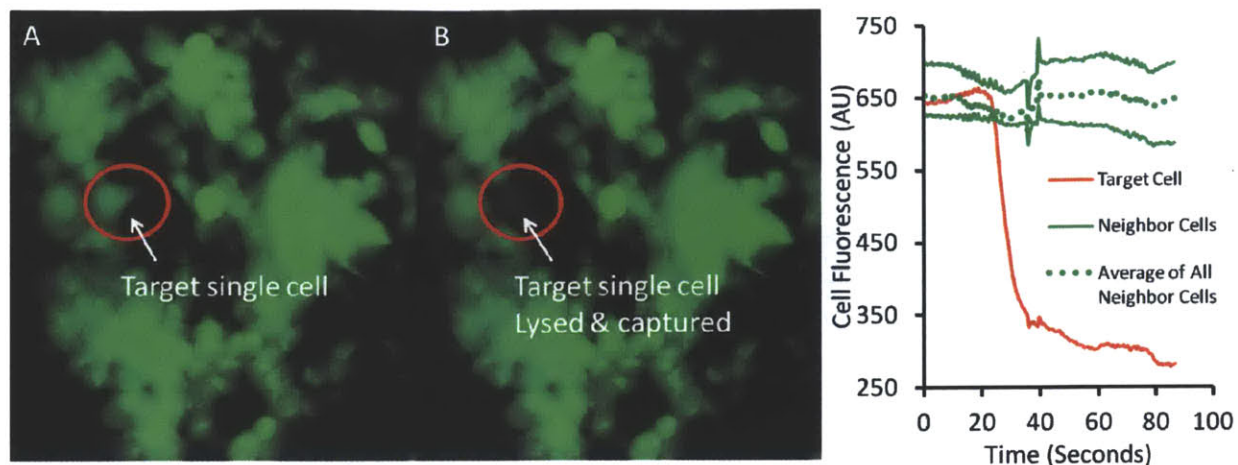


Figure 4.3 A selected single fluorescently labeled MCF-7 cell is lysed and its contents are captured using the microfluidic probe by flowing out a lysis buffer (with 1% Triton-X 100) and simultaneously flowing the cell lysate back into the device. Due to the limited lysis zone, other contacting and nearby cells even on a tissue culture dish grown to about $\sim 95\%$ confluence remain unaffected. A picture (A) before and (B) after lysis is shown and (C) the variation of cellular fluorescence during the lysis and capture is quantified.

engulfs and lyses the target cell while the other cells remain unaffected. The flow of the cell lysate back into the chip without dispersion is ensured by the high local fluid velocity inward. The radius of the lysis zone is similar to the width of the channels used which is nominally $50\mu\text{m}$ here. A further optimized version of the microfluidic probe with a smaller lysis zone ($\sim 10\mu\text{m}$) was used to demonstrate selective single cell lysis from a confluent tissue culture plate as shown in Figure 4.3. The variation of the fluorescence of the target cell as it is lysed and that of unaffected neighboring cells is shown in Figure 4.3c.

4.3 Integrated Microfluidic Probe v1

The single cell lysate flowing in from the probe tip can be used to perform any single cell biochemical assay after mixing it with appropriate assay or capture agents. Here we intend to mix it with fluorogenic peptide kinase substrates [10] which can either be directly observed or concentrated using a biomolecular concentrator [12] for sensitivity enhancement. Also

fluorescently labeled peptide substrates can be used which can then be separated based on their electrophoretic mobility and concentrated simultaneously in a concentration-enhanced mobility shift assay [18].

Measuring Kinase Activity in Cell Lysates: Compatibility of Lysis/Assay Components

Existing work [10] uses relatively dilute cell lysate (7.5%) in assays. However here, in order to use the single cell lysate (which is 50% lysate + 50% tissue culture medium) with minimum further dilution, we try to establish the compatibility of device components and the assay with the lysis agents at higher concentrations. It was observed (Figure 4.4a) that surface-patterned Nafion which we have used (see Section 3.2) as a cation-selective material to build bio-molecule concentrators was dissolved by the presence of 1% Triton-X 100 and to a lesser but still damaging extent even with detergent concentrations down to atleast 0.05%. Other non-ionic

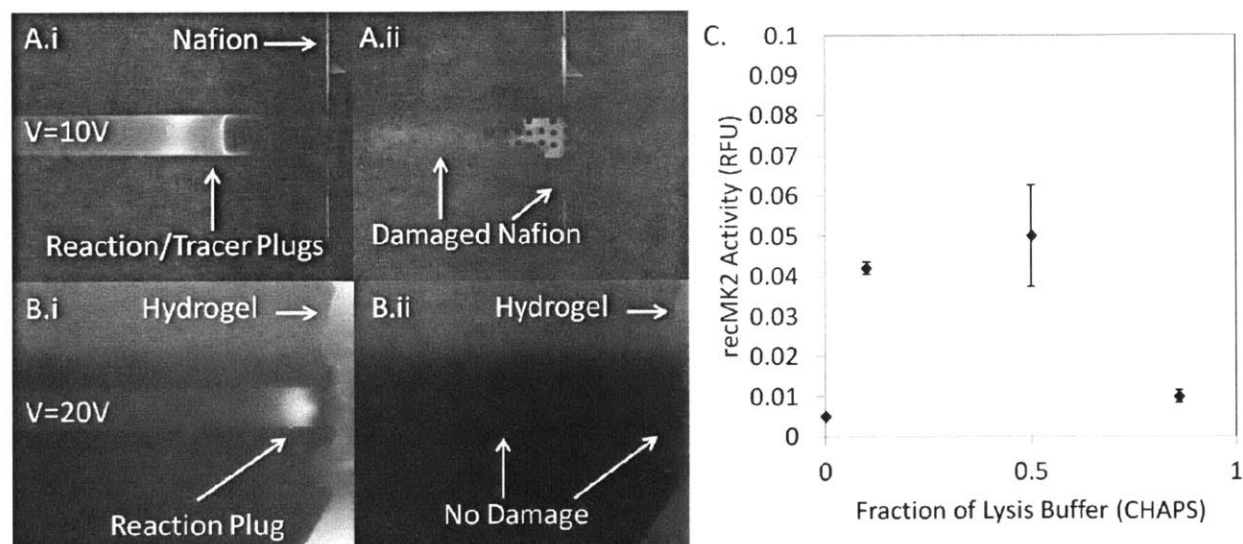


Figure 4.4a Nafion membrane before (i) and after (ii) damage due to presence of 1% Triton-X 100 in the buffer. b. Hydrogel membrane is not damaged by the same buffer. c. MK2 activity is inhibited both at zero and high (1%) lysis buffer concentration.

detergents such as Tween-20 were found to cause similar damage while ionic detergents such as the anionic detergent SDS or the zwitter-ionic detergent CHAPS were found to not cause any such damage, presumably because they were excluded from the membrane due to charge effects. Also anionic hydrogel [19], an alternative cation-selective material was found to be not affected by 1% Triton-X 100 Figure 4.4b.

The kinase assay itself was found (Figure 4.4b) to require a small amount of detergent (0.1X lysis buffer/0.1% detergent was the lowest tested) presumably to keep proteins suspended [20]. This rules out the use of Nafion with this assay except if a large post-assay dilution step is built in as was done off-chip by Cheow *et al* [18]. The assay was also inhibited in 1X lysis buffer conditions, presumably due to denaturing of proteins by the high detergent concentration [21] or incompatibility of some other lysis buffer component with the assay. This rules out direct use of the lysate for the assay and necessitates an on-chip dilution step with at least 5X dilution to bring the lysate concentration down to 10% which was found to work reliably and this motivated the chip design developed here onwards. Later it was also found that the Sodium Pyrophosphate, a component present in the lysis buffer as a phosphatase inhibitor, specifically forms a precipitate in presence of Magnesium Chloride, an essential component of the assay. Leaving the pyrophosphate out from the lysis buffer is thus a potential option for an assay without any dilution step which was not pursued here but is explored further later in a simpler proposed device (Section 4.9).

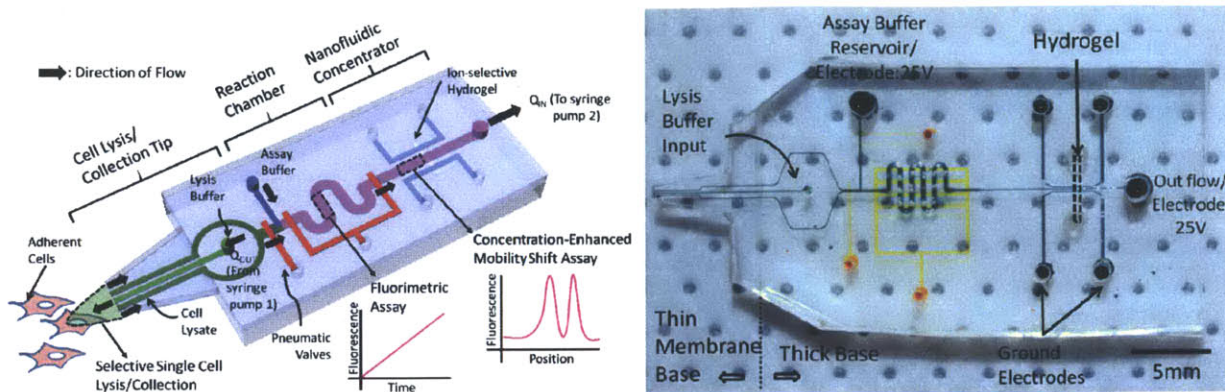


Figure 4.5a. The integrated microfluidic probe consists of three modules: cell lysis/collection tip to selectively lyse and collect single cells, a reaction chamber to mix and hold assay reagents and a nanofluidic concentrator to concentrate product peptides and perform a mobility-shift assay for phosphorylated/unphosphorylated substrates. **b.** Fabricated PDMS device showing the different layers: top piece with two layers: the valve lines (orange) and the channels (blue/green), bonded to bottom piece with two layers: a thin membrane base in the tip region and a thicker base which holds the UV-cured ion-selective hydrogel (dotted lines).

Development of Integrated Microfluidic Probe

An integrated microfluidic probe was developed that consists of the cell lysis tip, a dilution and assay reagent reservoir and channel, a reaction chamber with pneumatic valves to isolate it for observation and a hydrogel-based biomolecule concentrator to perform concentration-enhanced assays (Figure 4.5a). The fabricated device shown in Figure 4.5b, thus consisted of four layers: two in the top PDMS piece which consisted of the valve lines and microfluidic channels respectively and two in the bottom PDMS piece which consisted of the membrane base of the tip and the thicker base of the rest of the chip which held the anionic hydrogel pattern. Each of the pieces was thermally bonded internally while the two pieces were assembled by plasma-bonding.

The operation scheme of the device and the setup used are depicted in Figure 4.6a. Cell lysis and capture are done with the chip mounted on a micromanipulator which allows positioning next to single cells. After the cell lysate flows back into the chip and mixes with the

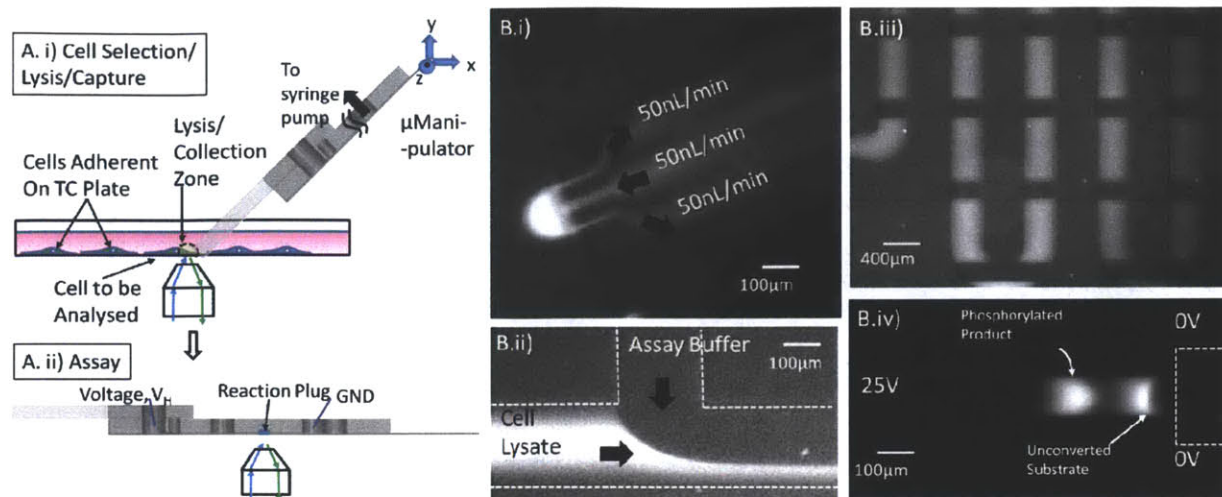


Figure 4.6 a. Scheme of operation with i) cell selection, lysis and capture with the chip mounted, slanted, on a micromanipulator and ii) assay with the chip mounted flat on a microscope stage for observation **b.** Device operation: i) a stable tunable lysis zone outside the tip as lysis buffer is flowed out/back in ii) collected cell lysate mixes with the kinase-specific substrate in assay buffer iii) valves are closed to capture the reaction mixture which is observed over time or iv) flowed into the concentrator for a mobility shift assay.

pre-loaded assay buffer simultaneously flowing in from the reservoir containing it and reaches the reaction chamber, the pneumatic valves are actuated to isolate it. The chip is then removed from the micromanipulator, wiped of any remaining tissue culture medium on the tip and placed on the microscope stage for observation and further manipulation of the reaction chamber contents within the chip. The complete operation of the device, visualized using buffers fluorescent proteins is shown in Figure 4.6b.

Single Cell Kinase Assay Demonstration

HepG2 cells adherent on 60 mm tissue culture plates were serum-starved for at least 12 hours before the assay and then stimulated using 300mM sorbitol which is known to activate MK2. Cells were then labeled with the fluorescent dye Cell Tracker Orange (as per the dye manufacturer's recommendation). Single cells from a tissue culture plate were lysed, mixed with

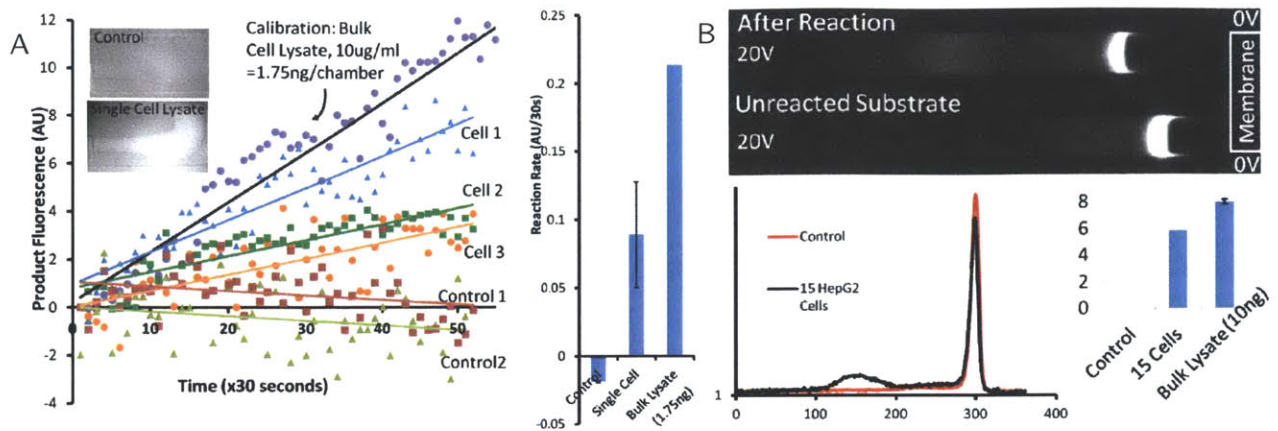


Figure 4.7a. Single cell MK2 Assay - Single sorbitol-stimulated, CellTracker Orange labeled HepG2 cells were lysed and the captured lysate was mixed with a MK2 substrate that shows increased fluorescence upon phosphorylation. Valves were closed and the chamber fluorescence recorded over time. Measured single cell activity corresponds well to the activity measured from a comparable amount (~ 1.75 ng) of bulk cell lysate as these cells have about ~ 1 ng/cell of total protein. **b.** Concentration-enhanced mobility shift Akt assay - A small group (~ 15) of HepG2 cells was lysed using the microfluidic probe and the lysate was reacted in the chamber with a fluorescent substrate. Products were diluted out and loaded into a multiplexed concentrator chip along with a negative control (unconverted substrate). A 5.8% phosphorylation was measured which compares well to corresponding amount of bulk lysate.

assay reagents and captured into the microfluidic probe. Observation of the reaction chamber over time revealed that single cell sensitivity was approachable in the direct fluorimetric assay without further concentration-enhancement. Single cell MK2 activation assays were performed with multiple single cells, the results of which are shown in Figure 4.7a. The assay sensitivity was calibrated with bulk, stimulated HepG2 cell lysate and the activity measured from single cells was found to equivalent to that from about ~ 1 ng of cell lysate which is roughly the expected total protein content of single cells of this kind. Given these promising results which were obtained without much any device design optimization, we further optimize this device for direct fluorimetric assay without concentration-enhancement (Section 0).

A demonstration of concentration-enhanced mobility shift assay from ~ 15 HepG2 cells was also performed in a two-chip format where the reaction products from the microfluidic

probe were diluted out and loaded into a multiplexed concentrator chip with a negative control and a bulk lysate calibration control. The simultaneous concentration and separation of the phosphorylated and unphosphorylated peptides allowed a ratiometric measurement of the phosphorylation level which was found to compare well between the cells and the corresponding amount of bulk lysate.

4.4 Optimization of Microfluidic Probe for Higher Sensitivity, Repeatability and Throughput

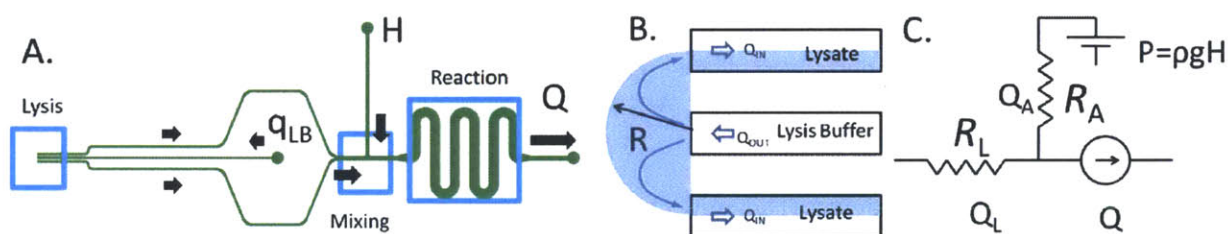


Figure 4.8a. Modular representation of the integrated microfluidic probe **b**. The radius of the lysis zone is controlled by the fluid velocity at the tip which is thus limited to a certain minimum before diffusion dominates. **c**. A circuit model of the mixing ratio showing the tip resistance, R_L and flow rate Q_L , the assay buffer channel resistance, R_A and flow rate Q_A and the assay buffer reservoir pressure P and total flow rate Q .

The microfluidic probe was optimized by considering its various modules as shown in Figure 4.8a and optimizing each subject to constraints offered by the operation of all the modules together. The sensitivity of the microfluidic probe is dependent on lysate concentration which depends on the volume into which the single cell is lysed. This is in turn, governed by the lysate flow rate Q_L and the time of lysis T_L so that the volume of single cell lysate V_L is: $V_L = Q_L \cdot T_L$. Lysis time, T_L is found to be relatively independent of flow rates and hence the lower the flow rate Q_L , lower the dilution of the lysate and potentially higher the sensitivity at this stage. The lower bound to this is set by the fact that the radius of the small lysis zone

depends on a high enough fluid velocity at the probe tip to overcome lysis agent and lysate diffusion Figure 4.8b. Thus we reduce the channel height at the tip from $15\mu\text{m}$ to $5\mu\text{m}$ to maintain a high fluid velocity with a lower flow rate.

The sensitivity is also proportional to the optical path length offered by the reaction chamber and thus its height is increased from $15\mu\text{m}$ to $30\mu\text{m}$. Thus a two-level chip is proposed with a tall chamber region and short probe region.

The repeatability of the assay was found to be hindered primarily by the variability of the mixing ratio which was found to vary due to the change in assay buffer height as it was consumed over time as shown in Figure 4.9a. This could be rectified by reducing the contribution of the gravity-driven assay buffer flow to the total flow by increasing the channel resistances as predicted by a simple circuit model of the mixing system:

$$\frac{Q_A}{Q_L} = \frac{\frac{P}{Q} + R_L}{-\frac{P}{Q} + R_A}$$

This can be achieved again by the reduction of the channel heights in the probe and

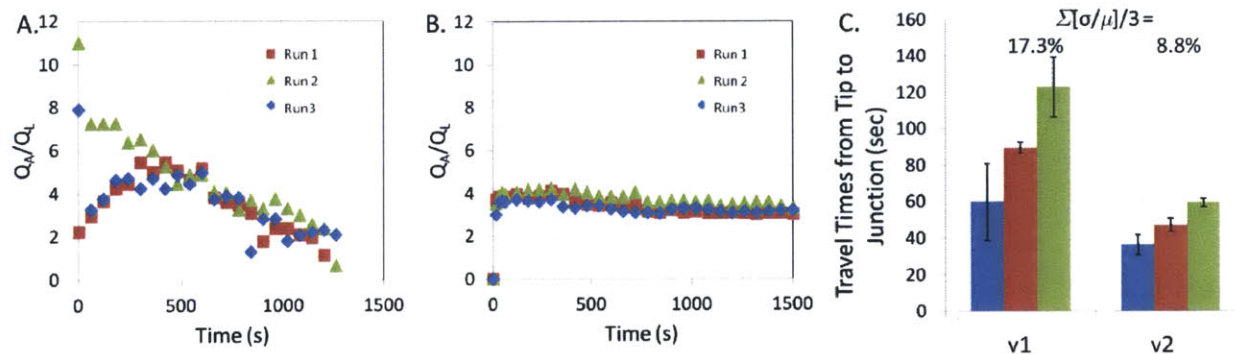


Figure 4.9a. The mixing ratio in the microfluidic probe was found to vary over time due to assay buffer depletion and resultant fluid height change. **b.** This effect was minimized by increasing channel resistances which reduced the relative contribution of the height-driven flow **c.** The chip-to-chip repeatability was also improved due to this.

assay buffer channel region to $5\mu\text{m}$ as described earlier. This was observed to improve repeatability of the mixing ratio over time in a single chip and also from chip to chip to within acceptable limits ($<10\%$) (Figure 4.9c). It was observed that repeatability in a single chip over experimental runs was still better than chip-to-chip repeatability. This indicated that probing multiple cells using the same chip would provide excellent technical repeatability of the assay. This would provide higher assay throughput too.

4.5 Integrated Microfluidic Probe v2

A new version of the microfluidic probe incorporating the design changes proposed above was fabricated as shown in Figure 4.10. This version features four reaction chambers which can be independently controlled using pneumatic valves. A valve controller was designed and made (Figure 4.11) to ease the use of this device. The flow in the device could thus be directed from the tip and assay buffer chamber to any of the four reaction chambers (Figure 4.11) and this control can be performed manually or via computer programs.

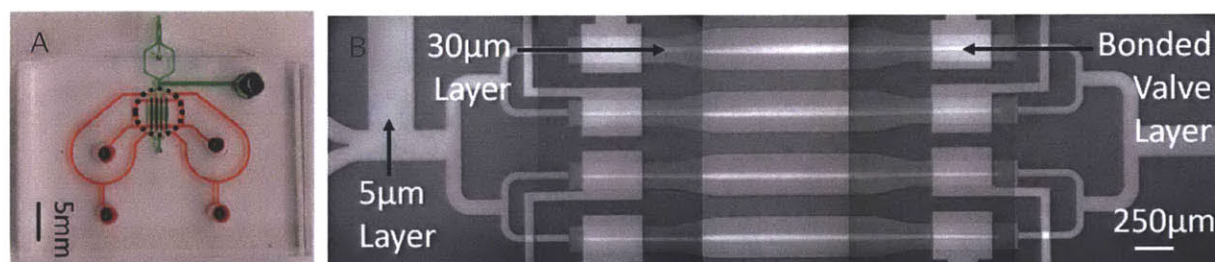


Figure 4.10a. Fabricated multiplexed microfluidic probe showing the two layers: (green) flow channels and (red) valve lines **b.** Micrograph of the inset area showing the reaction chambers controlled by the pneumatic valves. The flow channels are $5\mu\text{m}$ tall while and the reaction chambers are $30\mu\text{m}$ tall.

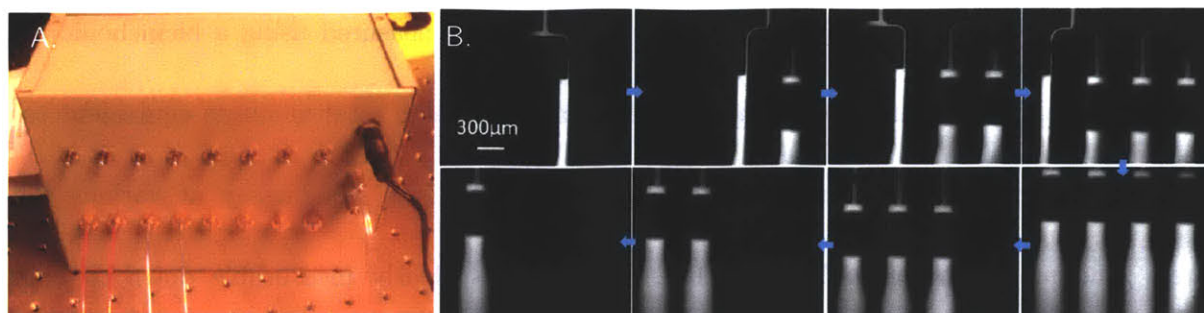


Figure 4.11a. Valve controller which can switch eight gas lines between the two input pressure levels either manually or via computer control. **b.** Filling and draining of the multiple reaction chambers of the microfluidic probe with, visualized using a fluorescent dye.

The chamber-to-chamber repeatability of the kinase assay was verified by probing a single sample of recombinant kinase MK2 four times, loading each of the four chambers with reaction mixtures. All four chambers were found to show similar fluorescence Figure 4.12 and reasonable agreement ($<10\%$ error) was found between the reaction rates measured from them.

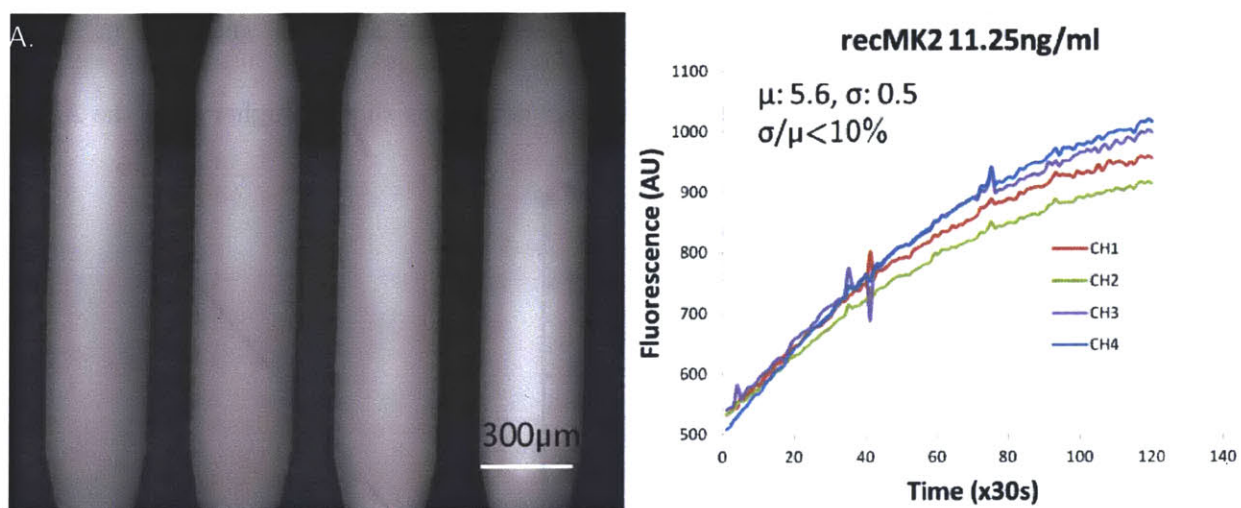


Figure 4.12a. Reaction chambers show uniform fluorescence at the end of a multiplexed assay in which each chamber was used to probe the same recombinant kinase MK2 sample. **b.** The product curves for the four reactions shown in a.

Kinase Assay Sensitivity Calibration

A calibration of the MK2 assay sensitivity in these chambers (volume: 18nL each) was performed by probing a bulk lysate of stimulated HepG2 cells stimulated using Sorbitol. The

total protein concentration in this lysate was independently measured using a bicinchonic acid assay (BCA) and the appropriate dilutions were made to mimic total amounts equivalent to a single cell and multiples or fractions thereof. The result of the MK2 assay at various total protein amounts is shown in Figure 4.13a. Activity was clearly measurable down to about 0.25ng of total protein and was found to linearly increase with the amount of total protein. Assuming that a single cell contains about 1ng of total protein, this indicates that MK2 activity from 1/4th of a cell should be measurable.

Similarly a calibration of the Akt assay sensitivity was performed using a bulk lysate of HepG2 cells stimulated using Insulin. The result of the Akt assay at various protein amounts is shown in Figure 4.13b. Again, assuming around 1ng/cell, this indicates that Akt activity from less than half a cell should be measurable. Comparing MK2 and Akt activities in similar amounts of bulk lysate shows that the measured MK2 activity is slightly higher than the Akt

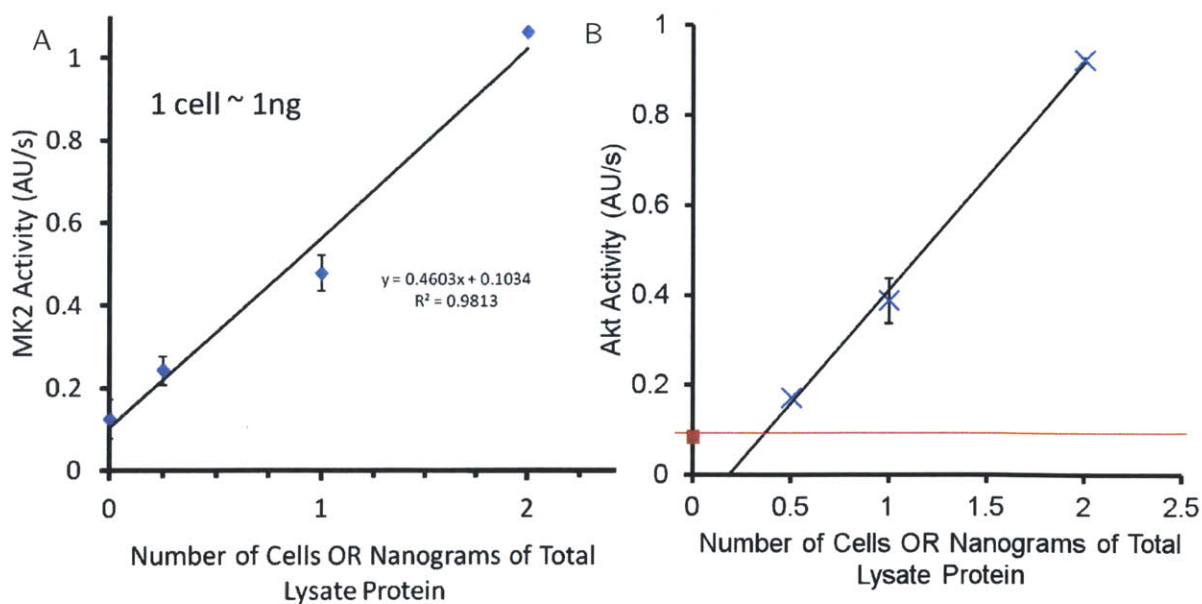


Figure 4.13a MK2 assay calibration curve obtained by probing bulk lysate of HepG2 cells stimulated using Sorbitol. **b.** Akt assay calibration curve obtained by probing bulk lysate of HepG2 cells stimulated using Insulin

activity. This is different from what is seen on probing these same bulk cell lysates on a plate reader where the measured MK2 activity is much higher than the measured MK2 activity (data not shown). One can only speculate as to the reasons for this – potentially the PDMS microchannel impedes the MK2 reaction somehow by maybe non-specific binding of either the enzyme or the substrate. This is worth further investigation as it might lead to further increased sensitivity if this issue is resolved.

4.6 Single Cell Kinase Activity Measurements

Single Cell MK2 Activity Measurement

A single cell MK2 assay was performed with Sorbitol-stimulated HepG2 cells, the result of which is shown in Figure 4.14. An around 10-fold higher reaction rate compared to earlier (Figure 4.7) was observed as a result of the lower volumes into which the cell lysate was diluted

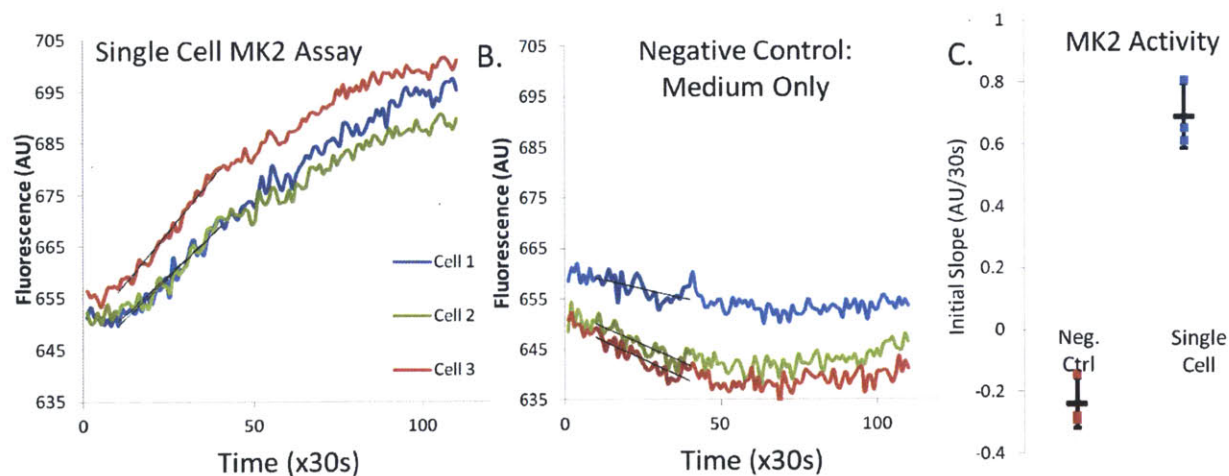


Figure 4.14a. Product curves obtained for the measurement of MK2 activity from single sorbitol-stimulated HepG2 cells show a repeatable positive slope. **b.** Product curves obtained for the measurement of MK2 activity from a negative control which consisted of tissue culture medium and lysis buffer only. **c.** Initial slopes of product curves from a and b show the ability to clearly distinguish MK2 activity in single cells from negative control.

as a result of chip optimizations. This was clearly distinguishable from the negative slopes obtained due to photo-bleaching from the negative control samples which consisted of tissue culture dishes with medium but without cells and thus collected a mixture of medium and lysis buffer. Also the single cell MK2 activity compares well to that measured from 1ng of bulk lysate (Figure 4.13a).

Single Cell Akt Activity Measurement

Single cell Akt activity measurements were performed on HepG2 cells. Figure 4.15 shows the results of probing single serum-starved and insulin stimulated cells for Akt activity. The measured single cell activity levels between these two conditions are clearly distinguishable as shown and compares well with to that measured from 1ng of bulk lysate (Figure 4.13a). It can also be noted here that the measured single cell kinase activities are higher for Akt than for MK2. This too, as noted above in Section 4.5 for the bulk lysate calibration assays, is the opposite of what is seen for bulk Akt and MK2 assays on plate readers.

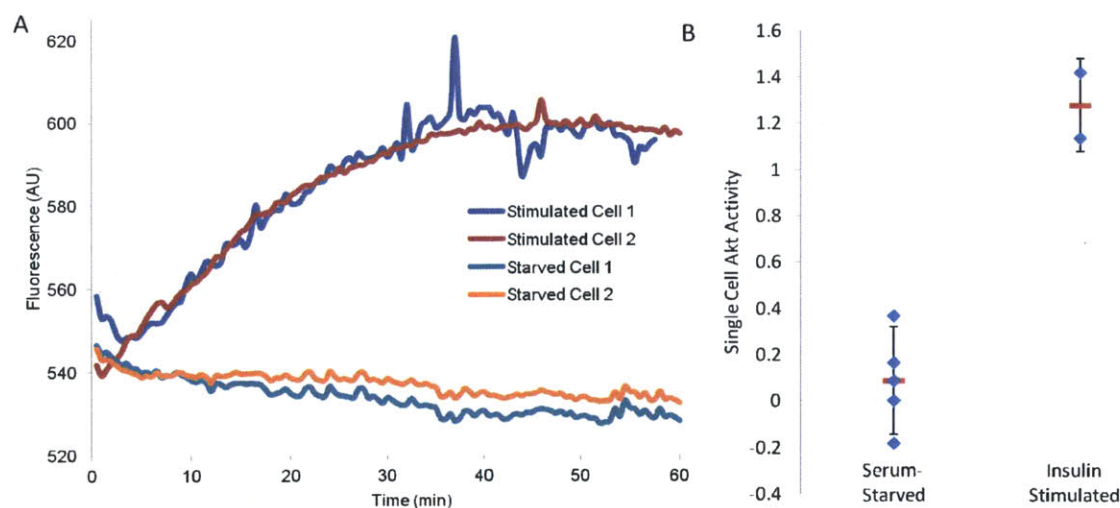


Figure 4.15a Product time curves for the measurement of Akt activity from single serum-starved and insulin stimulated cells **b.** Akt activity of serum-starved and insulin-stimulated single cells is clearly distinguishable

Time-course of Kinase Activation

We measured the time-course of activation of the kinase, MK2 by measuring its activity in single HepG2 cells stimulated by sorbitol (300mM) for different amounts of time. As shown in Figure 4.16a, an increasing level of single cell MK2 activity above the level measured in serum-starved cells was observed up to at least thirty minutes of stimulation which matches the corresponding time course of MK2 activation observed in bulk HepG2 cell lysate measurements.

The time course of Akt activation upon 500ng/ml insulin stimulation was also similarly measured. Again, an increasing level of Akt activity was seen extending to at least thirty minutes of stimulation (Figure 4.16b). While bulk Akt activity measurements from high cell density plates in the same cells have shown transient activation peaking at ~5-10 minutes of stimulation (data not shown), there is an earlier report showing [22] showing that Akt activation dynamics in MCF10A cells is cell density dependant and cells show sustained activity when plated at lower densities. This also correlates with the observation that the number of cell-cell contacts may affect the level to Akt activity with cells with lower cell-to-cell contact

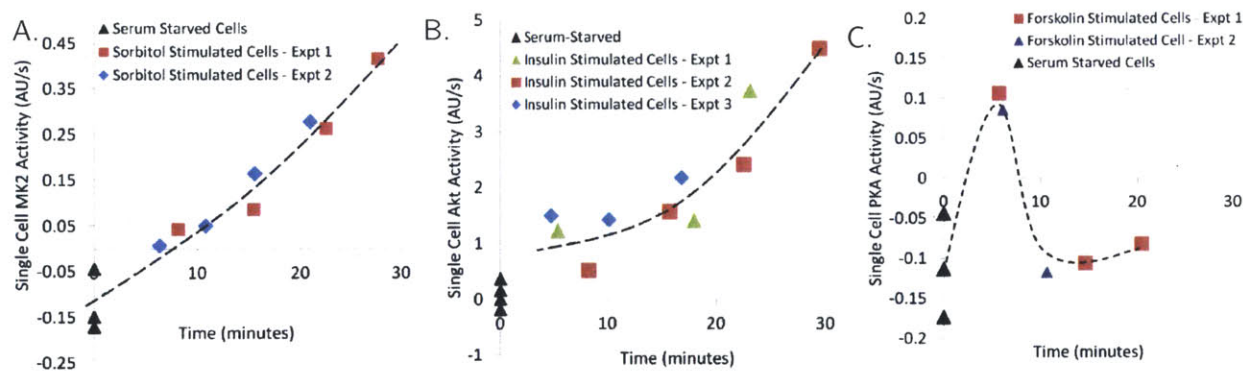


Figure 4.16a. Time course of MK2 activation measured from single cells stimulated with 300mM sorbitol for different amounts of time **b.** Time course of Akt activation measured from single cells stimulated with 500ng/ml insulin for different amounts of time. **c.** Time course of PKA activation measured from single cells stimulated with 25 μ M forskolin for different amounts of time

showing higher Akt activity [23]. This needs to be compared and corroborated with bulk HepG2 lysate measurements at cell densities comparable to those used for the single cell measurement.

We measured the time-course of activation of the kinase, PKA similarly by stimulating cells with $25\mu\text{M}$ forskolin. In this case a transient stimulation of PKA activity was observed peaking at about 5 minutes. This needs to be compared and corroborated with bulk HepG2 lysate measurements.

Correlating Extracellular Context and Cellular Phenotype to Kinase Activity

The microfluidic probe enables the selective assay of single adherent cells from specific extracellular contexts or those displaying specific phenotypes. We have observed an inverse correlation with cell density, of single cell Akt activity in HepG2 cells after 15 minutes of insulin stimulation Figure 4.17a. While cells plated at 10^4 cells/[60cm dish] and 10^5 cells/[60cm dish] have measurable Akt activities, those at 10^6 cells/[60cm TC dish] have no Akt activity above that of serum-starved cells. While these preliminary measurements were performed in different dishes plated to different densities, a potentially more interesting measurement suggested by

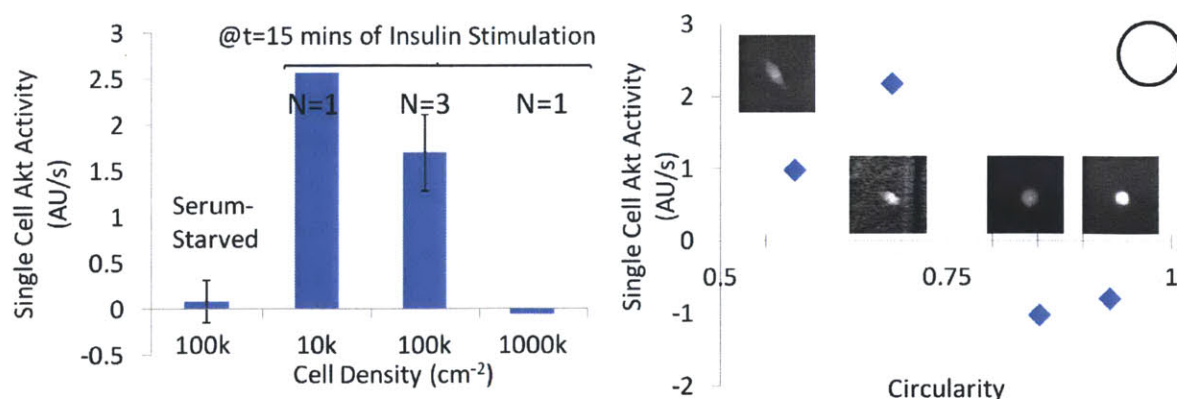


Figure 4.17a. Single cell Akt activity at 15 minutes of insulin stimulation for different cell densities. Akt activity was found to decrease with increasing cell density **b.** Single cell Akt activity vs cell circularity. Rounded cells (circularity nearer to 1) show no Akt activity while cell spread out cells show measurable Akt activity.

this results is one where the local cell density variation on a single plate could be correlated with the measured Akt activity. Whether global cell density of the whole dish or the local cell density near the cell being studied, controls the Akt activity would be interesting to find out.

Cell shape and morphology are simple yet important phenotypic markers. Here we observed that, on the same dish among neighboring cells – some cells are more rounded compared to others that show a more spread out shape. With the microfluidic probe, we find that the spread out cells show Akt activity while the rounded cells show no measurable Akt activity Figure 4.17b. Presumably the rounded cells are not well-attached to the surface or are about to die and this is reflected in the activity of Akt which is a know proliferative signal. Such cell-shape correlations can be a subject of further study.

4.7 Deconvolving Technical and Biological Variability in Single Cell Kinase Activity Measurements

Establishing that the measured variability among single cells is indeed biological variability and not a technical artifact is essential for further use of the microfluidic probe. The bulk kinase activity assays normalize the measured activity across experiments using a measurement of total protein in the cell lysate. Many other protein measurement techniques such as western blotting measure a so-called “house-keeping” protein as a loading control to overcome effects of unequal protein loading in different gel lanes. Here we develop an assay for measuring the activity in single cells of the metabolic enzyme Glyceraldehyde 3-Phosphate Dehydrogenase which is known to be expressed at a high level in most cells and is commonly used as a loading control in other

techniques. The sensitivity of this assay in the microfluidic probe was verified and calibrated using a bulk lysate of HepG2 cells. The results of this are shown in Figure 4.18a. Both serum-starved and insulin stimulated cells were seen to yield similar reaction rates. This is as expected since there is no known interaction at least in this cell type between the insulin activated pathways and GAPDH. A demonstration of the single cell GAPDH activity measurements is shown in Figure 4.18b. Further results for measurements of GAPDH activity in single cells are shown in Figure 4.18c along with a negative control from which they are clearly distinguishable.

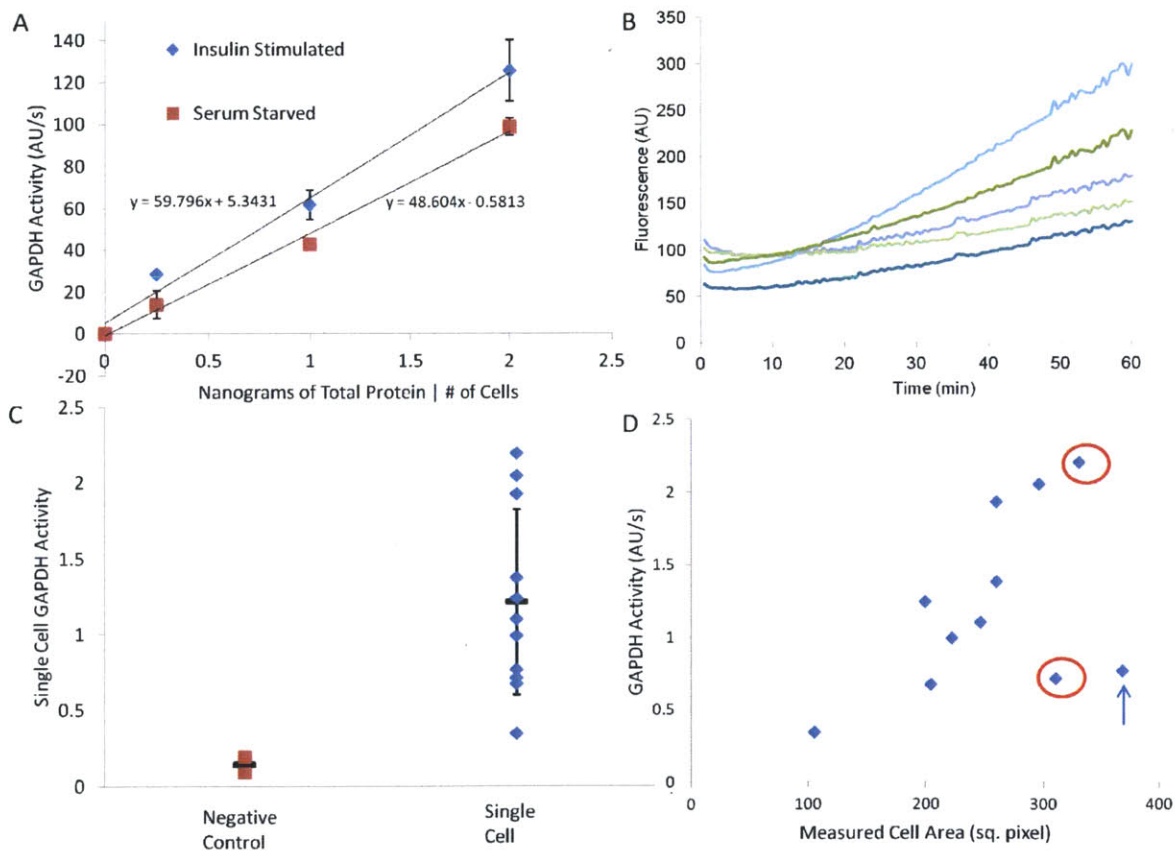


Figure 4.18a. Calibration of GAPDH assay using bulk lysate of serum-starved and insulin-stimulated HepG2 cells. **b.** Product curves obtained for the measurement of GAPDH activity from single HepG2 cells. **c.** Single Cell GAPDH Assay: Ability to measure GAPDH activity in single HepG2 cells as clearly distinguishable from a lysis buffer negative control is demonstrated. **d.** A correlation is seen between the measured single cell GAPDH activity and the cell size as estimated by the measured area of the cell. Red circles indicate potentially two cells or cells about to divide. The blue arrow shows a single cell with abnormally spread out morphology and hence the large area.

Further as shown in Figure 4.18d, a correlation between the cell size of the adherent single cells as estimated by the measured area (in sq. pixels) and the measured single cell GAPDH activity is observed. Red circles indicate potentially two cells or cells about to divide. The blue arrow shows a single cell with abnormally spread out morphology and hence the large area.

4.8 Integrated Microfluidic Probe v3: Measuring Multiple Kinase Activities from Single Cells

Given the sensitivity of the microfluidic probe as demonstrated by the ability to measure kinase activity from 0.25ng of total lysate protein (Figure 4.12c), we developed a further advanced version to measure simultaneously the activity of four enzymes from a single cell. This device is shown in schematic in Figure 4.19a and works by splitting the single cell lysate into

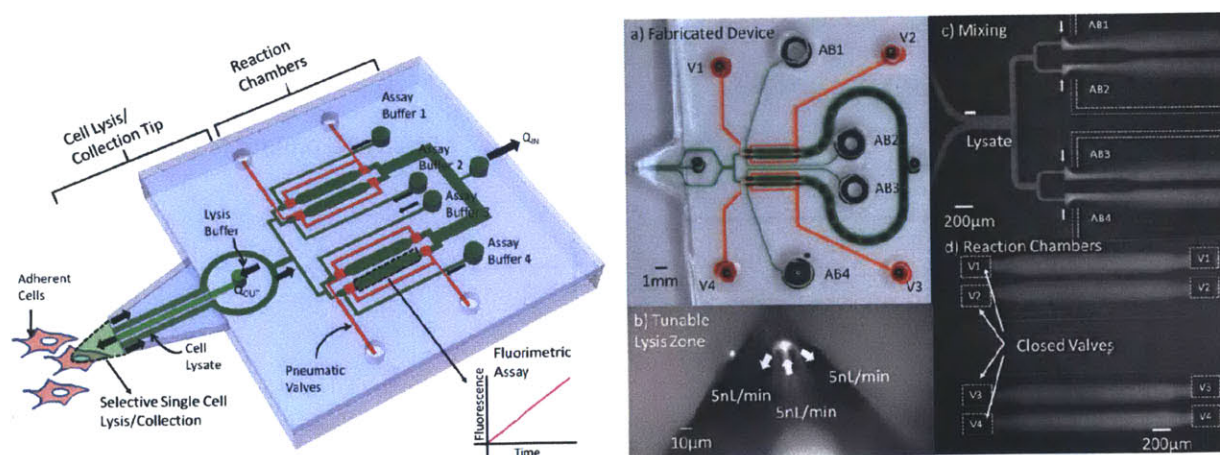


Figure 4.19a. The integrated microfluidic probe consists of two modules: cell lysis/collection tip to selectively lyse and collect single cell contents and a set of four reaction chambers in which the lysate can be mixed with different assay reagents and held for observation to measure activities of different kinases. **b.** a) Fabricated two layer PDMS device: top 5mm layer with channels and chambers (green) and lower 30 μ m layer which forms the base of the tip and contains the valve lines (red). b) Formation of lysis zone at tip c) Mixing of cell lysate with different assay buffers d) Reaction chambers filled and valves closed.

four parts and mixing each part with a different assay buffer into a different reaction chamber which can then be observed for activity over time. All the flows are controlled using pneumatic valves as before. The device and its operation are shown in Figure 4.19b.

We first use this device to perform two repeat measurements each of a single kinase from a single cell. The result, in Figure 4.20c, shows that two MK2 measurements from the same single cell are almost perfectly correlated. We also measure MK2 and GAPDH simultaneously from a single cell to establish repeatability and the absence of loading effects. These results are shown in Figure 4.20a. As seen here there is a small correlation between these two measurements potentially due to cell size or loading effects. Normalizing the measured MK2 activity to the measured GAPDH activity does explain some but not all of the variability of the data as shown in Figure 4.20b. This data needs to be supplemented with further repeat experiments in order for any robust conclusion to be drawn.

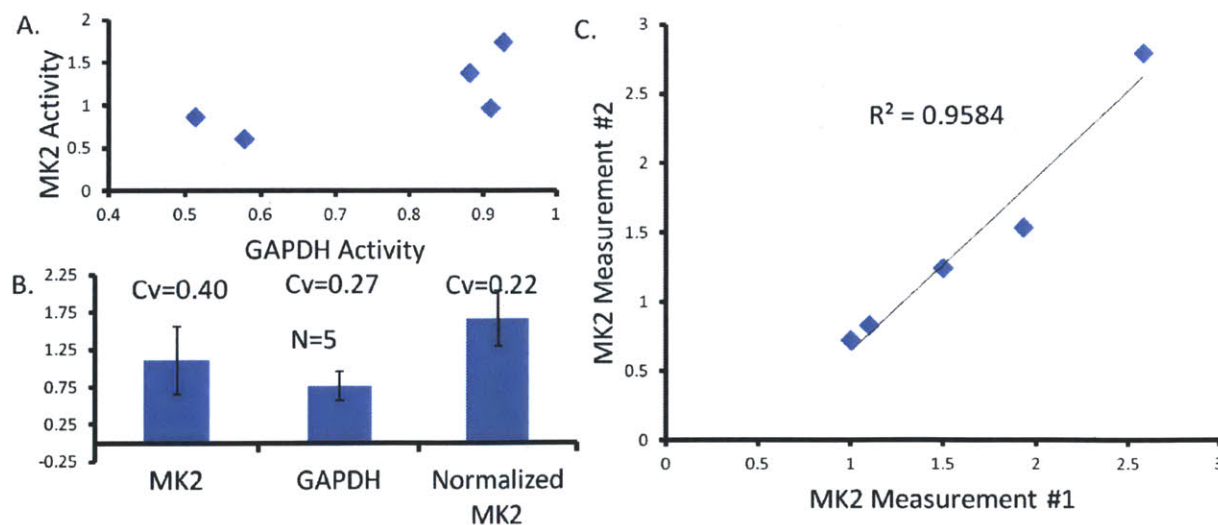


Figure 4.20a. Simultaneous measurement of MK2 and GAPDH activity in single HepG2 cells. **b.** Normalization using GAPDH activity reduces the observed variation only slightly **c.** Two MK2 measurements from the same cell are almost perfectly correlated.

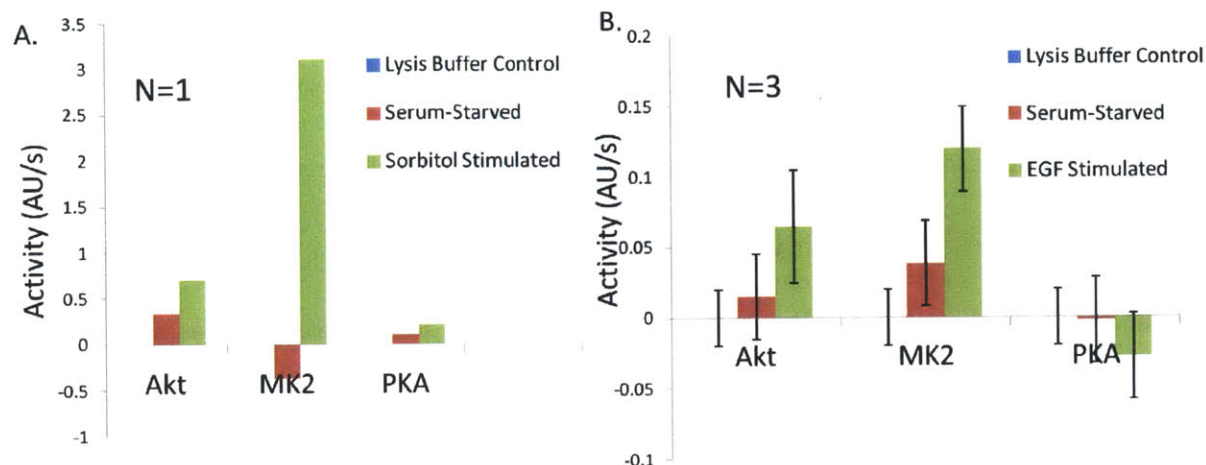


Figure 4.21a. Measurement of three kinase activities from a single Sorbitol stimulated HepG2 cells shows an activation of only MK2. **b.** Measurement of three kinase activities from three single EGF stimulated HepG2 cells shows an activation of Akt and MK2.

This device also can be used to simultaneously measure three kinases and the loading control enzyme, GAPDH thus providing a normalized kinase activity profile across different single cells. The measurement of three kinase activities simultaneously from single cells under various stimulation conditions is shown in Figure 4.21. Sorbitol stimulation is seen to activate MK2 selectively while EGF stimulation activates both Akt and MK2. Again, this data needs to be supplemented with further repeat experiments in order for any robust conclusion to be drawn.

4.9 Conclusions and Future Directions

In conclusion, we have demonstrated that the integrated microfluidic probe developed here can be used to selectively lyse and capture the contents of selected single cells and measure single or multiple kinase activities in them with or without other the activities of other enzymes as loading control. We demonstrated that while an integrated concentration-enhanced assay can be performed, a direct fluorimetric assay in a small volume chamber suffices to measure the

kinase activity from single cells and can in fact measure this activity from 1/4th of a cell. The time courses of kinase activation were measured by probing different single cells. A preliminary demonstration of correlations of extracellular context such as cell density and cell phenotypic measures such as cell shape with kinase activity was performed. A multi-kinase version of the microfluidic probe was developed and it was demonstrated to be able to measure up to four different enzymes simultaneously. These results suggest the directions of future work.

Correlating Phenotype or Extracellular Context with Kinase Activity Profile

Using the single kinase, multi-cell measurement probe (v2: Section 4.5) to pursue further measurements especially those that correlate single cell phenotype or extracellular context to its kinase activity seems to be of immediate interest. An example of an important biological process that involves a cell morphology change is the epithelial-mesenchymal transition (EMT). The microfluidic probe can enable the measurement of differences in kinase or other enzyme activities in neighboring cells that may or may not have undergone the EMT process and thus help in understanding this process which plays a critical role in cancer metastasis.

Further Improvements to Microfluidic Probe

The microfluidic probe can be further optimized especially to improve throughput. A three-layer design instead of the current two-layer design will enable the implementation of more complex architectures such as a multi-cell, multi-kinase device. Sensitivity can be further improved too further reducing the probe size and hence flow rates. The reliability of the microfluidic probe can also be further improved especially with regards to lysis buffer delivery which is currently – due to the thin channel and the low flow rate – especially prone to clogging

and flow rate oscillations. A potential solution to this is establishing a pressure-driven flow instead of using a syringe pump. This would allow faster starts and stops of this flow without oscillations.

Publications and Acknowledgements

Parts of this chapter have been published before in conference proceedings which are listed here as references [24, 25]. MCF-7 cells were obtained from the Voldman lab. HepG2 cells were obtained from the Lauffenburger lab. The experiments in Figure 4.4a and the development of the GAPDH assay were performed by Dr. Sarah Kolitz and some of the single cell kinase measurement results reported here were obtained in experiments performed with her. The experimental results in Figure 4.9 were obtained by Monica Lin. The valve controller was designed based on a design by Dr. Allison Skelley (Voldman lab).

4.10 References

- [1] S. J. Altschuler and L. F. Wu, "Cellular heterogeneity: do differences make a difference?," *Cell*, vol. 141, pp. 559-63, May 14 2010.
- [2] M. Niepel, *et al.*, "Non-genetic cell-to-cell variability and the consequences for pharmacology," *Current Opinion in Chemical Biology*, vol. 13, pp. 556-561, 2009.
- [3] A. Loewer and G. Lahav, "We are all individuals: causes and consequences of non-genetic heterogeneity in mammalian cells," *Curr Opin Genet Dev*, vol. 21, pp. 753-8, Dec 2011.
- [4] B. Snijder and L. Pelkmans, "Origins of regulated cell-to-cell variability," *Nat Rev Mol Cell Biol*, vol. 12, pp. 119-25, Feb 2011.
- [5] J. M. Irish, *et al.*, "Single Cell Profiling of Potentiated Phospho-Protein Networks in Cancer Cells," *Cell*, vol. 118, pp. 217-228, 2004.
- [6] N. Kumar, *et al.*, "Quantitative analysis of Akt phosphorylation and activity in response to EGF and insulin treatment," *Biochemical and Biophysical Research Communications*, vol. 354, pp. 14-20, 2007.
- [7] A. Y. Ting, *et al.*, "Genetically encoded fluorescent reporters of protein tyrosine kinase activities in living cells," *Proceedings of the National Academy of Science*, vol. 98, pp. 15003-15008, 2001.

- [8] G. D. Meredith, *et al.*, "Measurement of kinase activation in single mammalian cells," *Nature Biotechnology*, vol. 18, pp. 309-312, 2000.
- [9] A. Proctor, *et al.*, "Metabolism of peptide reporters in cell lysates and single cells," *Analytst*, vol. 137, pp. 3028-38, Jul 7 2012.
- [10] M. D. Shults, *et al.*, "A multiplexed homogeneous fluorescence-based assay for protein kinase activity in cell lysates.," *Nature Methods*, vol. 2, pp. 277-283, 2005.
- [11] C. I. Stains, *et al.*, "Interrogating signaling nodes involved in cellular transformations using kinase activity probes," *Chem Biol*, vol. 19, pp. 210-7, Feb 24 2012.
- [12] J. H. Lee, *et al.*, "Microfluidic Concentration-Enhanced Cellular Kinase Activity Assay," *Journal of the American Chemical Society*, vol. 131, pp. 10340-10341, 2009.
- [13] D. Di Carlo, *et al.*, "Single-Cell Enzyme Concentrations, Kinetics, and Inhibition Analysis Using High-Density Hydrodynamic Cell Isolation Arrays," *Analytical Chemistry*, vol. 78, pp. 4925-4930, 2006.
- [14] D. Juncker, *et al.*, "Multipurpose microfluidic probe," *Nat Mater*, vol. 4, pp. 622-628, 2005.
- [15] R. D. Lovchik, *et al.*, "Micro-immunohistochemistry using a microfluidic probe," *Lab Chip*, vol. 12, pp. 1040-3, Mar 21 2012.
- [16] A. Ainla, *et al.*, "A Microfluidic Pipette for Single-Cell Pharmacology," *Analytical Chemistry*, vol. 82, pp. 4529-4536.
- [17] E. Lukovic, *et al.*, "Monitoring protein kinases in cellular media with highly selective chimeric reporters," *Angew Chem Int Ed Engl*, vol. 48, pp. 6828-31, 2009.
- [18] L. F. Cheow, *et al.*, "Concentration-enhanced mobility shift assays with applications to aptamer-based biomarker detection and kinase profiling," in *15th International Conference on Miniaturized Systems for Chemistry and Life Sciences (μ TAS 2011)*, Seattle, USA, 2011, pp. 1023-1025.
- [19] P. Kim, *et al.*, "Stabilization of ion concentration polarization using a heterogeneous nanoporous junction," *Nano Letters*, vol. 10, pp. 16-23, 2010.
- [20] M. D. Womack, *et al.*, "Detergent effects on enzyme activity and solubilization of lipid bilayer membranes," *Biochim Biophys Acta*, vol. 733, pp. 210-5, Sep 7 1983.
- [21] W. W. Womack, *et al.*, "Psychoeducational courses for a nonpatient clientele at a mental health center," *Hosp Community Psychiatry*, vol. 34, pp. 1158-60, Dec 1983.
- [22] C. M. LeVea, *et al.*, "EGF-dependent cell cycle progression is controlled by density-dependent regulation of Akt activation," *Exp Cell Res*, vol. 297, pp. 272-84, Jul 1 2004.
- [23] T. L. Yuan, *et al.*, "Cell-to-cell variability in PI3K protein level regulates PI3K-AKT pathway activity in cell populations," *Curr Biol*, vol. 21, pp. 173-83, Feb 8 2011.
- [24] A. Sarkar, *et al.*, "An Integrated Microfluidic Probe for Concentration-Enhanced Selective Single Cell Kinase Activity Measurement," in *15th International Conference on Miniaturized Systems for Chemistry and Life Sciences (μ TAS 2011)*, Seattle, Washington, USA, 2011, pp. 1394-1396.
- [25] A. Sarkar, *et al.*, "An Integrated Microfluidic Probe for Multiplexed Single Cell Kinase Activity Measurement," in *16th International Conference on Miniaturized Systems for Chemistry and Life Sciences (μ TAS 2012)*, Okinawa, Japan, 2012.

Chapter 5 Conclusions and Future Work

5.1 Thesis Contributions

In this thesis, we set out to develop microfluidic and nanofluidic tools for sensitive enzyme activity assays that could approach single-cell enzyme activity measurement and perform reliable cell signaling measurements in presence of cellular heterogeneity.

We have developed several such tools using broadly two confinement principles: electrical trapping of charged molecules into \sim pL-scale plugs in the biomolecule concentrator and mechanical confinement in small volumes using either \sim pL-scale water-in-oil droplets or \sim nL-scale chambers formed using pneumatic valves.

We have also demonstrated the measurement of various cellular enzymes ranging from secreted extracellular proteases (MMP-9) to intracellular kinases (Akt, MK2, PKA and metabolic enzymes (GAPDH). The intracellular enzymes were measured simultaneously or separately from single cells and the possibility to correlate the variations in their activity with the variation in extracellular context and single cell phenotype was demonstrated.

The specific contributions of this thesis can be summarized thus:

- The non-linear enhancement of enzymatic reaction kinetics in the biomolecule concentrator was experimentally studied and modeled. It was shown that the measured rates are linear in enzyme concentration. Also it was shown that concerns of the

enhancement of off-target reactions due to substrate accumulation are mitigated by a substrate-limited phase reached by the reaction over long times.

- A new linear enhancement mode of enzymatic reaction kinetics in the biomolecule concentrator was proposed in which the reaction follows the accumulation and occurs in a separate enclosed volume. This was demonstrated by integration with an integrated chamber with pneumatic valves or with a microfluidic water-in-oil droplet generator. The droplet device was further used for multiplexed measurement of activity of secreted proteases in cellular supernatants.
- A microfluidic probe was developed which can selectively lyse visually selected single cells and capture their contents in small volumes for sensitive on-chip measurement and manipulation. The integration of this probe with a fluorimetric assay chamber and a concentration-enhanced assay using a biomolecule concentrator was demonstrated.
- An optimized, multiplexed microfluidic probe was developed which can lyse multiple cells and measure kinase activities in them using a direct fluorimetric assay was developed. Measurement of the activity and the time-course of activation of kinases: Akt, MK2 and PKA were demonstrated using this probe. The measurement of single cell GAPDH activity was also demonstrated.
- A multiplexed microfluidic probe which can measure multiple kinase and other enzyme activities from single cells was developed and demonstrated.

5.2 Directions for Future Work

The various sensitive enzyme assay methods developed here are well-suited for and ready to be applied to a number of interesting biological and other problems.

The non-linear yet controlled enhancement of enzyme activity afforded by the biomolecule concentrator opens up several opportunities for very high sensitivity detection. This can be applied with slight modifications to problems ranging from biomarker discovery to diagnosis of diseased states in which low abundance enzymes are bio-markers to the detection of bacterial contaminants in water for human consumption. The linear enhancement tools developed here are directly applicable to high throughput measurement of enzyme kinetics and thus are potentially applicable to drug and drug target testing especially for low-abundance targets.

The microfluidic probe is a versatile tool that can be used to interface standard tissue culture platforms to microfluidic systems. Assays can thus be performed at both scales depending on their suitability to particular formats and the results can then be correlated at the single cell scale. The immediate prospect of this tool seems to be in correlating single cell phenotype of local cellular microenvironment variability to intracellular signaling state via kinase activity measurement. However the system is agnostic to specific assay chemistry and various other assays: enzymatic, binding-based or even PCR-based assay can be easily implemented without much modification and can benefit from the interfacing capabilities and high sensitivity afforded by small volumes.